University of Texas Rio Grande Valley
ScholarWorks @ UTRGV

Theses and Dissertations

8-2022

Synthesis and Processing of Polymeric Materials for Hydrogen Storage

Dominic Adrewie
The University of Texas Rio Grande Valley

Follow this and additional works at: https://scholarworks.utrgv.edu/etd

 Part of the Chemistry Commons

Recommended Citation

Adrewie, Dominic, "Synthesis and Processing of Polymeric Materials for Hydrogen Storage" (2022). *Theses and Dissertations*. 1003.
https://scholarworks.utrgv.edu/etd/1003

This Thesis is brought to you for free and open access by ScholarWorks @ UTRGV. It has been accepted for inclusion in Theses and Dissertations by an authorized administrator of ScholarWorks @ UTRGV. For more information, please contact justin.white@utrgv.edu, william.flores01@utrgv.edu.

SYNTHESIS AND PROCESSING OF POLYMERIC MATERIALS FOR HYDROGEN STORAGE

A Thesis

by

DOMINIC ADREWIE

Submitted to the Graduate College of the

Requirements for the degree of

MASTER OF SCIENCE

Major Subject: Chemistry

The University of Texas Rio Grande Valley

August 2022

SYNTHESIS AND PROCESSING OF POLYMERIC MATERIALS FOR HYDROGEN STORAGE

A Thesis
by
DOMINIC ADREWIE

COMMITTEE MEMBERS

Dr. Javier Macossay-Torres
Chair of Committee

Dr. Tülay Ateşin
Committee member

Dr. Shervin Fatehi
Committee member

August 2022

Copyright 2022 Dominic Adrewie

All Rights reserved

ABSTRACT

Adrewie, Dominic, Synthesis and processing of polymeric materials for hydrogen storage. Master of Science (MS), August, 2022, 59 pp, 1 table, 35 figures, references, 83 titles.

Hydrogen is one of the most promising clean alternative fuel sources, but it has faced several hurdles to adoption, including storage and transportation issues. Several methods have been proposed and developed, and they are steadily being improved. Key among these is the use of polymers as safe hydrogen storage media.

This work investigated the polymerization of methyl vinyl ketone using different concentrations of 2,2'-azobis(2-methylpropionitrile) (AIBN) as the initiator in a free radical polymerization mechanism. Fourier transform Infrared (FTIR) and Nuclear Magnetic Resonance (NMR) were used to confirm the formation of the polymer. The thermal properties of the polymers were then determined using thermogravimetric analysis (TGA) and differential scanning calorimetry (DSC). There was a subsequent analysis of the effect of the initiator concentration on the conversion rate, and also of the molecular weight of the polymers produced using gel permeation chromatography. Attempts were also made to create fibers using electrospinning and particles using nanoprecipitation to obtain a higher surface area polymer.

DEDICATION

I dedicate this thesis and my academic progress to the Jehovah God Almighty (by whose mercies I have made thus far) and to my parents whose hard work, selflessness, unwavering support, and prayers that has helped me through my education.

ACKNOWLEDGMENT

Sincere thanks go to Prof. Javier Macossay-Torres (my advisor) for his unwavering patience and guidance throughout my thesis, and to Dr. Victoria Padilla of the Engineering department for allowing the use of DSC and TGA instruments.

TABLE OF CONTENTS

Page

LIST OF FIGURES

Page

CHAPTER I

INTRODUCTION

Over the years, the increase in industrial activities coupled with an increasing world population has led to higher demand for energy resources (Shiva Kumar and Himabindu, 2019). In the 21st century, energy is one of the most important resources that will be needed for many applications to enhance human life and wellbeing. Energy in the form of electricity is now an integral part of society, and an important ingredient for human advancement, sustainability, and improvement. It is used for many purposes, ranging from domestic applications such as powering light bulbs, washing machines, dishwashers, television, and mobile phones, as well as industrial applications (Li *et al.*, 2014), such as manufacturing, cloud storage, and cryptocurrencies. Conventional ways of producing electricity have, however, led to the production of harmful chemicals that lead to environmental pollution and its consequences (Abdalla *et al.*, 2018).

One of the novel clean energy sources being explored is hydrogen (Wang *et al.*, 2016). Hydrogen, which is the lightest element on the periodic table (Kato and Nishide, 2018) with atomic number 1, has shown enormous potential (Zhao *et al.*, 2021), because it is a renewable energy source that is abundant and readily available. Furthermore, hydrogen combustion only releases water vapor. As a result, it is considered the most environmentally friendly energy source (Chen *et al.*, 2021). It is also the most efficient energy carrier, (Yadav and Xu, 2012) and it is estimated to produce an energy output per mass of at least three times that of conventional fuel (Zhu and Xu, 2015). Hydrogen is produced from various sources such as hydrocarbons

(mainly natural gas), coal, and biomass via a variety of techniques. Even though hydrogen is currently mainly sourced from non-renewable fossil fuels and the splitting of water, research has shown a huge potential for renewable sources such as biomass, solar, and wind power. There is, however, a challenge in terms of the storage and transportation of hydrogen, which has contributed to the slow adoption of hydrogen fuel as a viable alternative to conventional crude (Singla, Nijhawan and Oberoi, 2021).

CHAPTER II

LITERATURE REVIEW

Hydrogen and sources of hydrogen

In 1766, British scientist Henry Cavendish (1731–1810) demonstrated to the Royal Society of London that there were two sorts of air: “fixed air”, which is carbon dioxide, and “inflammable air”, which is hydrogen. By reacting zinc metal with hydrochloric acid, Cavendish created hydrogen gas. In the late 1770s, he demonstrated that hydrogen is significantly lighter than air and was the first to generate water by mixing hydrogen and oxygen with an electric spark (Grimes, Varghese and Ranjan, 2008). Hydrogen is the lightest element known to man, and it is abundant but rarely available as a pure element. Instead, it is found in association with oxygen in water, in combination with carbon in a variety of hydrocarbon fuels, and in plants, animals, and other forms of life. More than 70% of the Earth's surface is covered with hydrogen bonded in water and organic forms (Dunn, 2002). The gaseous form of hydrogen is the lightest gas (14 times lighter than air), highly flammable (emitting a colorless flame), and odorless. When used as a fuel, it provides more energy per unit mass than today's conventional fuels (Najjar, 2013). It takes energy to produce pure hydrogen, however, because it does not occur naturally, and thus it may serve as an energy carrier. When the hydrogen is consumed, the energy is converted to heat (Spath and Mann, 2003; Yasuda *et al.*, 2006; Lee *et al.*, 2013). Hydrogen created from water is predicted to gradually replace fossil fuels and become the primary energy carrier in the second half of the twenty-first century, according to the hydrogen economy concept. To this purpose, various technological issues must be resolved in order to ensure the safety of hydrogen

technologies and to improve hydrogen production, storage, and transportation techniques (Marchenko and Solomin, 2015).

Hydrogen fuel

Hydrogen is most frequently used as a fuel in the aerospace industry. For many years, propellants made of liquid hydrogen and oxygen have been utilized in a variety of applications. It has been discovered that a propellant mixture of liquid H_2 and O_2 releases the most energy per unit weight, which is an important factor in space applications. However, liquid hydrogen has not been used as a fuel in other applications, such as cars, due to the high cost of liquefaction, the difficulty of maintaining it as a liquid, and handling safety concerns.

Since H_2 is the cleanest burning fuel, there is a lot of interest in using it as a fuel in cars (Ramachandran and Menon, 1998; Crabtree and Dresselhaus, 2008). In comparison to methane and gasoline, hydrogen's physical and chemical properties allow for flammability under a wide array of conditions. As a result, hydrogen engines may operate on excessively lean mixes more successfully than gasoline engines. A flammable mixture can be created by mixing air with hydrogen to as little as 4% by volume. Compared to other fuels, hydrogen has a substantially lower ignition energy (0.02 MJ), higher diffusivity, and higher ignition temperature. Hydrogen can be ignited at a wide range of concentrations when contained, but it is very difficult to ignite when unconfined (Balat, 2008).

Hydrogen has an advantage over gasoline since it can diffuse in air much more readily. The simplicity with which a consistent mixture of fuel and air can be formed, as well as the quick dispersion of hydrogen when a leak first appears, are primarily responsible for this improved

mixing (Sharma and Ghoshal, 2015). When employed in an internal combustion engine, hydrogen's unusually low density causes two issues. They are: (1) a very large volume is required to store enough hydrogen to give a vehicle a sufficient driving range; and (2) the power output is decreased due to the lower energy density of a hydrogen–air mixture (Balat, 2008). Figure 2.1 shows a summary of hydrogen sources and uses as reported by Barilo and Loosen in the 2018 Green Transportation and Summit Expo (Barilo and Suzanne, 2018).

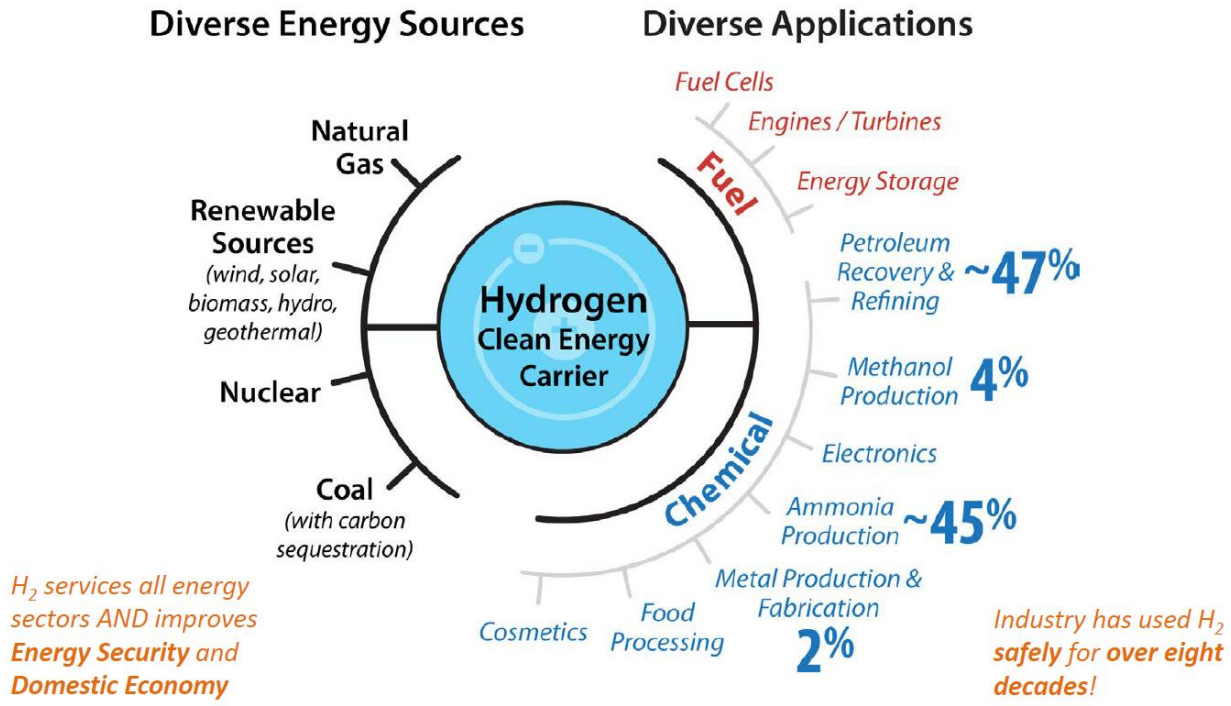

Figure 2. 1: Hydrogen sources and applications

Hydrogen storage

Hydrogen storage and transport, which is a key element in the development of a hydrogen economy (Bellosta von Colbe *et al.*, 2019), is currently a challenge due to various factors (Reardon *et al.*, 2012), (Oka *et al.*, 2021). These important challenges must be resolved before a technically and commercially successful hydrogen economy can be developed (Saeedmanesh, Mac Kinnon and Brouwer, 2018). Generally, hydrogen can be stored physically (in pure form) (Yang *et al.*, 2010) by adsorption or chemical storage (Andersson and Grönkvist, 2019). Cryogenic or high-pressure tanks are two common methods for storing and transporting hydrogen. However, because cryogenic tanks require cooling and thermal insulation, hydrogen storage is limited (Kato *et al.*, 2016). The liquefaction and continuous boil-off of hydrogen require a significant amount of energy. Tank walls must be relatively thick to increase the hydrogen density when compressing gaseous hydrogen to 70–80 MPa. Explosions (caused by collisions), hydrogen permeability, and embrittlement of the tank walls are all inherent safety hazards (Najjar, 2013).

To help alleviate some of the problems of storage, solid materials that chemically bind or physically adsorb hydrogen at volume densities greater than liquid hydrogen have become promising hydrogen storage techniques. The goal is to find a storage material that meets three competing criteria: high hydrogen density, reversibility of the release/charge cycle at moderate temperatures (in the 70–100°C range) to be compatible with today's fuel cells, and fast release/charge kinetics with minimal energy barriers to hydrogen release and charge (Crabtree and Dresselhaus, 2008). Although various materials have been discovered that meet one or two of the criteria, none have been demonstrated to meet all three. Aside from these fundamental

technical requirements, acceptable storage media must also meet cost, weight, longevity, and safety standards (Satyapal *et al.*, 2007).

Hydrogen holds huge potential as the main energy of the future and a very viable replacement for conventional fuel (Zivar, Kumar and Foroozesh, 2021) without posing a threat to the environment and humans, but storage and transport of hydrogen have presented severe challenges due to cost, efficiency, and the accompanying risk involved. There is therefore the need to develop new storage and transport approaches. There has been extensive research on the use of polymers as hydrogen storage and transport material due to their relatively large surface area (Kato and Nishide, 2018). Physisorption of hydrogen onto porous organic polymers and the reversible binding of hydrogen to these polymers are being extensively explored. which has shown a massive promise but still requires a lot of fine-tuning.

Electrospinning is a technique that affords porous fibers, so it is possible to obtain polymers that show promise for hydrogen storage while enhancing its capacity by forming porous materials, thus increasing the chemisorption of the polymers with higher physisorption (Müller and Arlt, 2013).Therefore, the approach of this proposal, as applied to hydrogen storage promises to be a safe and efficient approach to hydrogen storage and transport.

Hydrogen storage methods

Hydrogen storage methods can be classified under compression, liquefaction, physisorption, chemisorption, metallic hydrides, and complex hydrides.

Compression

The most common method for storing hydrogen is compression, which involves compressing hydrogen gas in high-pressure containers up to 80 MPa (Züttel, 2004). It is an expensive method due to material requirements for the storage containers, and this method also possesses a major safety concern (Yu, Hebling and Revathi, 2016),(Zhou, 2005).

Liquefaction

Liquefaction of hydrogen involves the cooling of hydrogen gas into liquid hydrogen in cryogenic containers. Liquid hydrogen can only be stored in cryogenic systems due to the low critical temperature of hydrogen (33 K), as there is no liquid phase above the critical temperature. At room temperature, the pressure in a closed storage system might reach 104 bar. Liquid hydrogen has a volumetric density of 70.8 kg m^3, which is slightly greater than solid hydrogen (70.6 kg m^3). The energy-inefficient liquefaction process and the thermal insulation of the cryogenic storage tank to reduce hydrogen boil-off are the problems of liquid hydrogen storage (Züttel, 2004).

Physisorption

Physisorption is an intriguing strategy for storing molecular hydrogen because its low enthalpy of adsorption/desorption makes hydrogen more readily accessible in ambient settings when compared to chemisorption, which requires temperatures on the order of 600 K for desorption. (Scanlon *et al.*, 2009). The physisorption of hydrogen possesses advantages like fast kinetics of adsorption and desorption, being completely reversible, and small enthalpy of

adsorption for molecular H_2 storage means only a small amount of heat is produced during onboard refueling (Hirscher, Panella and Schmitz, 2010). Porous materials such as carbon nanotubes and metal-organic frameworks are commonly used in physisorption (Bénard and Chahine, 2007),(Ding and Yakobson, 2015),(Panella, Hirscher and Roth, 2005) to maximize the storage capacity (Environ *et al.*, 2012). Adsorption in this case is due to Van der Waals forces.

Chemisorption

Chemisorption is a chemical process in which hydrogen attaches chemically to the storage medium in solid-state hydrogen storage. The hydrogen molecules disintegrate into hydrogen atoms, which occupy the material's interstitial site or matrix, forming new chemical bonds. Unlike hydrogen physisorption, the chemisorption process involves higher energies owing to the breaking and making of chemical bonds (Ren *et al.*, 2016). One of the drawbacks of chemisorption is that the process is usually not readily reversible (Chang, 2016). The products tend to be either too stable or unstable, the former making the process irreversible and the latter making degradation too easy. To make the reaction reversible, appropriate catalysts are being researched and used to ensure a minimum degree of reversibility (Ma *et al.*, 2020).

Metallic hydrides

Metallic hydrides are compounds in which metals are chemically bound to hydrogen. Therefore, any hydrogen compound bonded to a metallic element is effectively a metal hydride. The bond in metal hydrides is usually covalent, but ionic bonds are also possible (Young, 2018). A variety of factors influence the selection of metal hydride compounds for hydrogen storage and compression applications. First and foremost, the hydride synthesis and breakdown processes must be reversible within the operating temperature and hydrogen pressure ranges required for the application, and also, under the operating conditions, the material must have a

high reversible hydrogen storage capacity (Tarasov *et al.*, 2021). Metal hydride technologies are a promising choice for tackling hydrogen storage challenges because of their compactness, safety, simplicity, and versatility. The use of metal a hydride can give extremely high hydrogen storage capacity per unit volume (often even greater than liquid hydrogen), safety and reliability, and excellent purity of the H_2 delivered (Lototskyy *et al.*, 2015). Metal hydrides that can quickly supply hydrogen at room temperature typically have storage capacities of <2% by weight and cannot match the demands of a proton-exchange fuel cell in an automobile. Much of the present metal hydride research is focused on hydrides consisting predominantly of light elements in order to achieve high gravimetric capacities ($Z \leq 13$) (Graetz, 2009).

Complex hydrides

The term "complex" refers to molecules or ensembles generated by the interaction of ligands and metal ions. Complex hydrides, which may also be known as classic chemical hydrides (Aiello *et al.*, 1998) are usually metal complexes in which hydrogen is covalently bounded. Alanates, amides, and borohydrides (group I and II salts of $[AlH_4]^-$, $[NH_2]^-$, and $[BH_4]^-$) have recently attracted a lot of attention as prospective hydrogen storage materials. Although only the alanates include anionic metal complexes, all of these compounds are now referred to as "complex hydrides." Amides and borohydrides, like alanates, are ionic compounds in which hydrogen is covalently bound to core atoms in "complex" anions (Orimo *et al.*, 2007).

Polymers for hydrogen storage

A polymer is simply a very large molecule with high molecular weight, and which is formed from smaller units called monomers. The monomers may all be the same or may differ from one another, but all must be bifunctional. Polymer comes from the Greek words *poly* and *meros*, which signify many and pieces, respectively. Instead of polymer, some scientists prefer the term macromolecule, or huge molecule. Others argue that natural polymers, often known as biopolymers, and manufactured polymers should be examined separately. All polymers, however, follow the same principles (Carraher Jr., 2011).

Polymers are being extensively explored for use as hydrogen carriers and have seen significant progress over the years (Kato and Nishide, 2018). Polymers are being explored as physisorption and chemisorption storage media. These polymers include porous organic polymers, like hyper crosslinked polystyrene and porous cubic frameworks of $Zn_4O(CO_2)_6$ coordinated with an octahedral array of 1,4-benzenedicarboxylate and benzene tribenzoate groups (Kato and Nishide, 2018), and conducting polymers such as polythiophene, poly (para phenylenevinylene), polyaniline (PANI), polypyrrole (Ppy), poly (para phenylene), and polyacetylene (Mahato *et al.*, 2020), Poly (methyl vinyl ketone) is among the most recent polymers being explored for hydrogen storage potential (Oka *et al.*, 2021).

Poly (methyl vinyl ketone)

Poly (methyl vinyl ketone) is a polymer consisting of methyl vinyl ketone monomer.

Methyl vinyl ketone (MVK), also known by other names including vinyl methyl ketone, methylene acetone, 3-buten-2-one, 2-butenone, butenone, buten-2-one, and 1-buten-3-one, is a

molecule having the formula $CH_3C(O)CH=CH_2$ and the International Union of Pure and Applied Chemistry (IUPAC) name but-3-en-2-one. It is a reactive compound classed as an enone, and it is the most basic example of the class. It is a colorless, very hazardous flammable liquid with a strong odor (Siegel and Eggersdorfer, 2000). It is soluble in both water and polar organic solvents. Methyl vinyl ketone is used as an alkylating agent, a commercial starting material for plastics, a component of ionomer resins, and an intermediate in the synthesis of steroids and vitamin A (Larranaga, Lewis and Lewis, 2016). One of the earliest methods of creating poly (methyl vinyl ketone) was by reacting methyl vinyl ketone with 0.5% by weight benzoyl peroxide at 50–60 °C (Levesque, 1982).

Free radical polymerization

Free radical polymerization is a type of polymerization which is initiated by a free radical, typically a peroxy or azo compound. Between 1910 and 1930, the first free radical polymers were made by initiation with peroxy chemicals. Polymerization by redox processes was discovered separately and simultaneously in the 1940s in Germany and the United Kingdom. The systematic exploration of azo compounds as free radical initiators began in the 1950s (Braun, 2009). In 1937, Flory defined the kinetics of vinyl polymerization as a chain reaction involving free radicals and proposed that only bimolecular combination or disproportionation processes can terminate two active (growing) chains. Flory's article is the first comprehensive description of free radical polymerization, in which the overall rate Rw in reliance on monomer [M] and initiator [I] concentrations can be represented with the overall rate coefficient K: $Rw = K \cdot [M] \cdot [I]^{1/2}$ (square-root law) (Flory, 1937). In this research, a free polymerization reaction using an azo compound is carried out. The azo compound being used is azobisisobutyronitrile (AIBN).

AIBN, which has a designated IUPAC name 2,2'-azobis(2-methylpropionitrile) or 2-(azo(1-cyano-1-methylethyl))-2-methylpropane nitrile, is a white powder with chemical formula $C_8H_{12}N_4$ that is insoluble in water but soluble in alcohols and other organic solvents. It has a melting point of 376–378 K, density of 1.1 g/cm, and molar mass of 164.21 g/mol.

Above 313.15 K, AIBN decomposes to form a molecule of nitrogen gas and two 2-cyanoprop-2-yl radicals:

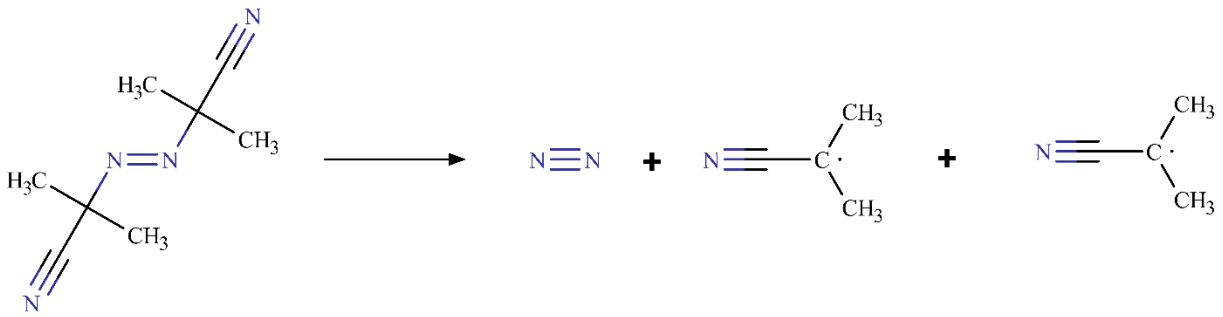

Figure 2. 2: Decomposition of AIBN

In most case, reactions with AIBN are done around 339.15–345.15 K (Clayden, Greeves and Warren, 2012). AIBN-derived radicals are commonly utilized in adhesives, acrylic fibers, detergents, and other products.

Free radical polymerization occurs in 4 steps, as illustrated in Figure 2.3: initiation, propagation, chain transfer, and termination. The initiation step involves the creation of radicals by the breakdown of an initiator, usually with the help of heat or light. The radical created attacks monomers and leads to creation of monomer radical molecules in the propagation step, followed by the chain transfer step where the monomer radicals attack other monomers/oligomers/polymers to form radicals of longer chain length. The reaction then comes

to a stop in the termination step, when two product radicals react with each other (Davis, 2005). This process is an example of a chain reaction.

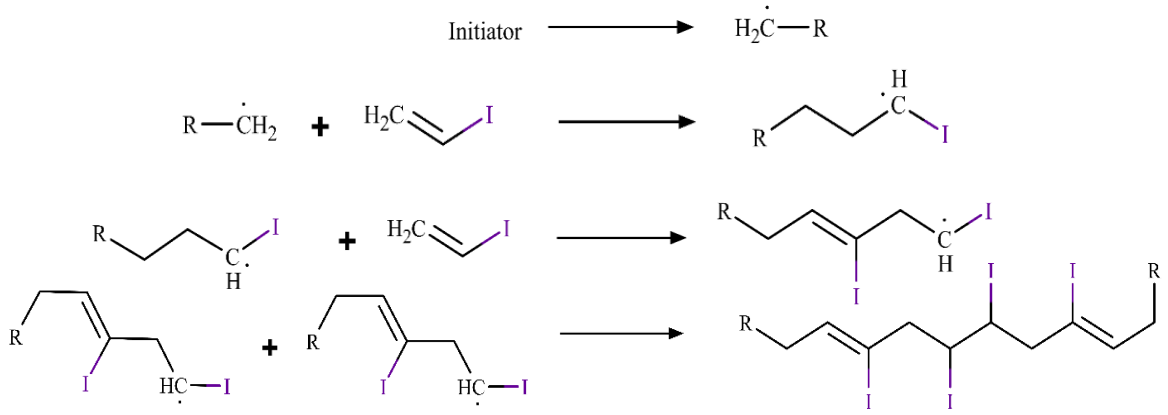

Figure 2. 3: Free radical polymerization process.

Characterization methods

Fourier Transform Infrared Spectroscopy (FTIR)

The absorption of infrared radiation by chemical bonds in a substance is measured by infrared spectroscopy. Functional groups, which are chemical structural fragments of molecules, absorb IR radiation in similar frequency ranges regardless of the structure of the rest of the molecule in which they are found (Buijs, 2006). Absorption bands are commonly reported in both frequency and wavelength units. Reciprocal centimeters (cm^{-1}), also known as wavenumbers, are frequency units that are equal to cycles per centimeter, and the recommended unit for expressing wavelength in infrared spectroscopy (Thompson, 2018). Microns (µ) and micrometers (µm) are wavelength units with identical numerical values. A molecule can only absorb radiation if the

frequency of the entering infrared radiation matches one of the molecule's fundamental modes of vibration. These vibrational modes include:

- Stretching—the process of increasing or decreasing the space between two atoms.
- Bending—in which an atom's location changes in relation to its original bond axis.
- Scissoring—the process of bending a molecule such that a bond angle decreases and increases.
- Rocking—in which a bond twists relative to several adjacent atoms (Thompson, 2018)

This means that only a small portion of the molecule's vibrational motion is altered, while the remainder of the molecule remains untouched. Infrared spectroscopic analysis was carried out with a Bruker Vertex 70 FT-IR spectrometer with single reflection diamond ATR and OPUS software.

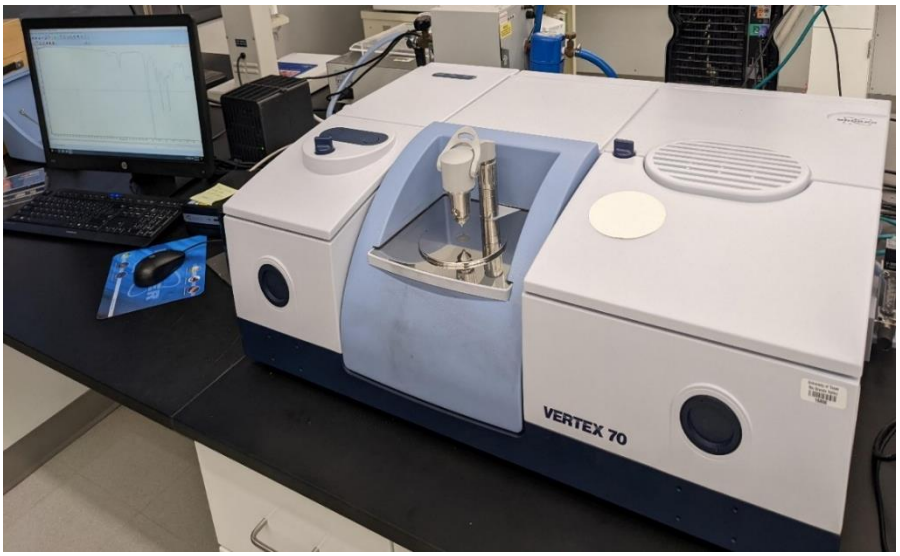

Figure 2. 4: Vertex 70 FTIR instrument

Gel Permeation Chromatography (GPC)

In 1964, J.C. Moore of the Dow Chemical Company investigated the process and coined the name gel permeation chromatography and the Waters Corporation was granted a license to use the patented column technology, which they commercialized in 1964 (Moore, 1964).

Gel permeation chromatography (GPC), also known as gel filtration chromatography (GFC) or size exclusion chromatography (SEC), is a chromatographic technique for fractionating macromolecules based on their molecular size (Gellerstedt, 1992) . It allows the molecular weight distribution of a polymer sample to be measured (Williams, 1970) and can be used for fractionation, purification, separation, and the determination of the quaternary structure of proteins. The stationary phase for GPC is a gel and in order to apply a gel to a specific separation, the pore size of the gel must be precisely managed. The absence of ionizing groups and low affinity for the chemicals to be separated in a particular solvent are other desired qualities of the gel forming agent (Waters, 2014). The type of gel used depends on the separation needs. Tetrahydrofuran (THF), o-dichlorobenzene, and trichlorobenzene are the most frequent GPC eluents for polymers that dissolve at room temperature. The varying permission rates of each solute molecule into the interior of the gel particles are the basis of gel filtration chromatography or gel permeation photography (GPP). It differs from other chromatographic techniques that rely on analytes' physical and chemical interactions. The porous beads put on the column determine the separation via gel filtration (Skoog, Holler and Crouch, 2016). There are 3 steps in GPC, which are:

1. Preparing the column, which is carried out by swelling the gel, packing the column with semi-permeable, porous polymer gel beads with a well-defined range of pore diameters, washing the

column with several volumes of buffer solution to remove any air bubbles, and testing column homogeneity.

2. Using a syringe to load the sample onto the column.

3. Eluting the sample and detecting the components.

The basic setup for GPC is shown in figure 2. 5.

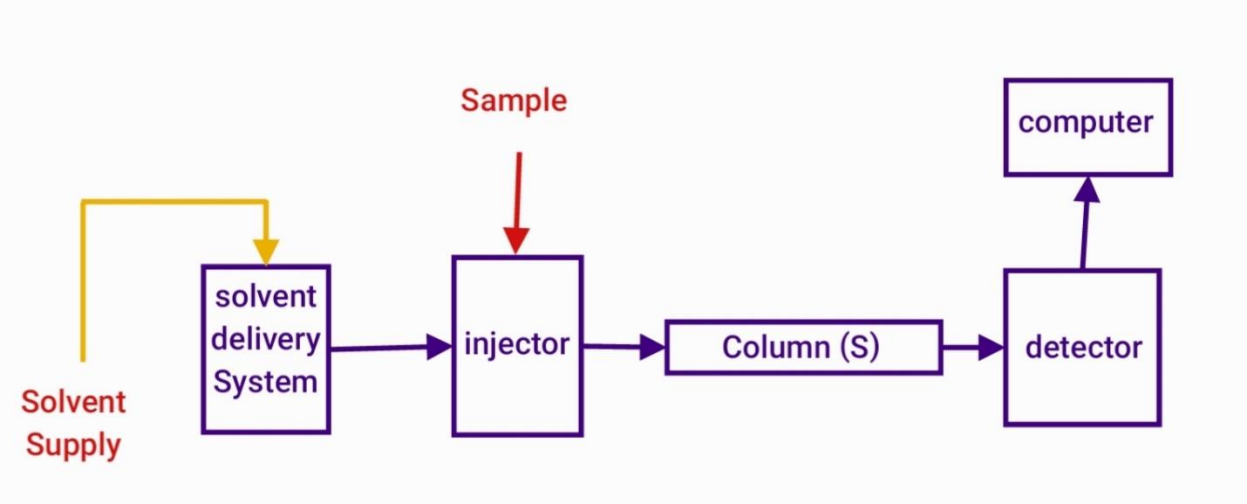

Figure 2. 5: Diagram of gel permeation chromatography setup

GPC is conventionally calibrated with accepted standards such as polystyrene, but a light scattering instrument can also be integrated and used for molecular weight determination. These light scattering instruments can use low-angle light scattering (LALS), right-angle light scattering (RALS), hybrid low-angle light scattering/right-angle light scattering (Hybrid LALS/RALS) or multi-angle light scattering (MALS). LALS measure light scattering at angles less than 10^{o}, RALS measure light scattering at 90^{o}, and MALS measure light scattering at multiple angles (Malvern Instruments Worldwide, 2013).

Thermogravimetric Analysis (TGA)

Another common method for polymer characterization is thermogravimetric analysis (TGA). As the sample specimen is submitted to a controlled temperature program in a controlled atmosphere, the weight change of the material is monitored as a function of temperature or time (Inan, 2017). TGA is an effective method for determining the thermal stability of materials, particularly polymers. Changes in the weight of a specimen are measured while its temperature is increased in this procedure (Sarfraz *et al.*, 2021). TGA can be used to determine the moisture and volatile content of a sample. The system comprises of a highly sensitive scale for measuring weight changes and a programmable furnace for controlling the sample's heat up rate. The balance is thermally separated from the heat and is positioned above the furnace (Ebnesajjad, 2011),(Tomoda *et al.*, 2020).

Differential Scanning Calorimetry

Differential scanning calorimetry (DSC) is a thermoanalytical technique that measures the difference in the amount of heat required to raise the temperature of both a sample and a reference as a function of temperature. Throughout the experiment, the sample and reference are kept at nearly the same temperature. The temperature program for a DSC study is usually set up so that the sample holder temperature rises linearly as time passes. Over the temperature range to be scanned, the reference sample should have a well-defined heat capacity.

Nuclear Magnetic Resonance Spectroscopy (NMR)

Nuclear magnetic resonance spectroscopy (NMR) is based on the energy difference between the spin states of the nucleus in the presence of a magnetic field, in contrast to the majority of typical spectroscopic techniques, which use electrons. Any NMR experiment requires the target nucleus to have a nuclear spin in order to function. Fortunately, many of the elements have spin-active stable isotopes. These include hydrogen, carbon, nitrogen, phosphorous, and fluorine (specifically ^{1}H, ^{13}C, ^{15}N, ^{31}P and ^{19}F) (Simpson, Simpson and Soong, 2018). A non-zero spin nucleus can align with the magnetic field in the presence of a magnetic field, which typically leads to a lower energy state, or it can align against the magnetic field, which typically leads to a higher energy state (Lysak, Simpson and Simpson, 2022).

The NMR experiment makes use of the energy difference between these two states to split energy in a phenomenon known as the Zeeman effect. All NMR experiments, from straightforward 1-D investigations to intricate multinuclear multidimensional NMR, start with manipulating the magnetization of the sample. The net magnetization, which may be changed by pulsing the sample with radiofrequency (RF) radiation, is produced when slightly more nuclear spins are aligned with the field than against it on average. In order to detect the magnetization, the magnetization must first be "flipped" from its equilibrium position (aligned with the external magnetic field) into a plane perpendicular to the magnetic field. Following this flip, the magnetization starts to precess around the magnetic field like a spinning top that has been pushed off axis. The resonant (or Larmor) frequency, which is specific to the chemical environment of the nucleus, is the frequency of this precession. NMR is an effective tool for identifying chemical structures and analyzing non-covalent interactions because of how sensitive the resonant frequency is to changing chemical environments (Singh and Singh, 2022).

Electrospinning

Electrospinning, a technique for fabricating continuous fibers in the submicron to nanometer scale that was built over the last decade (Jose Varghese *et al.*, 2019), is primarily reliant on strong electrostatic forces. Over the last decade, there has been a great rise in academic and commercial interest in employing electrical forces to generate polymer fibers with diameters ranging from 2 nm to several micrometers using polymer solutions of both natural and manmade polymers (Ahn *et al.*, 2006; Lannutti *et al.*, 2007; Reneker and Yarin, 2008). Electrospinning is a relatively stable and straightforward method for creating nanofibers from a wide range of polymers. Spun nanofibers also have a high surface area-to-volume ratio, tunable porosity, malleability to conform to a wide range of sizes and forms, and the ability to modify the nanofiber composition to achieve the required characteristics and usefulness. Electrospun nanofibers have been actively explored in recent years for use in a variety of applications, including filtration, optical and chemical sensors, electrode materials, and biological scaffolds (Liang, Hsiao and Chu, 2007).

A basic electrospinning system typically includes three key components: a high voltage power supply, a spinneret, and a grounded collection plate (commonly a metal screen, plate, or revolving mandrel) as shown in figure 2. 6.

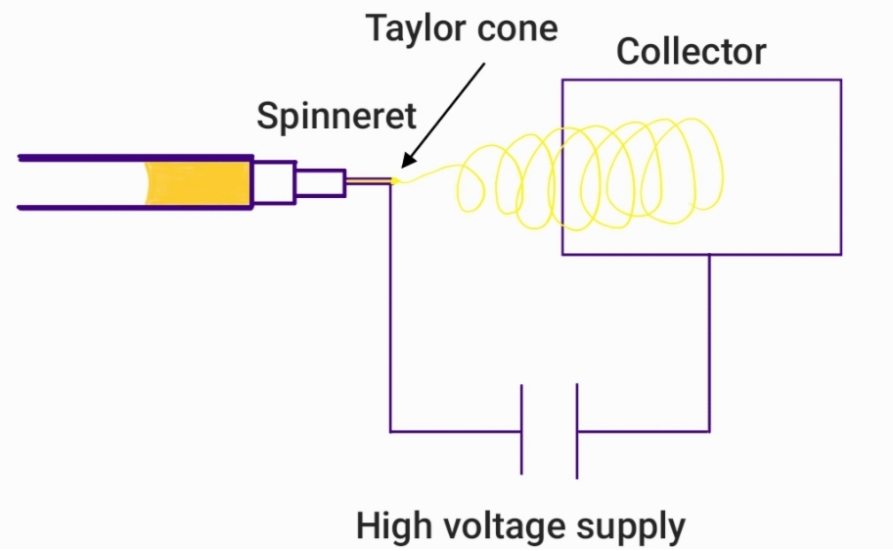

Figure 2. 6: Basic diagram of electrospinning setup

A suspended conical droplet is generated when a charged polymer solution is passed through the spinneret under an external electric field, with the surface tension of the droplet in equilibrium with the electric field. A small jet is released from the surface of the droplet and pulled toward the collecting plate when the applied electric field is strong enough to overcome the surface tension. The solvent in the jet stream gradually evaporates as it propagates toward the collecting plate (Huang *et al.*, 2003). During its transit to the collection plate, the electrically charged jet experiences a series of electrically induced bending instabilities, resulting in hyper-stretching. This stretching reduces the diameter of the jet leading to the deposition of dry micro or nano fibers on the collection plate (Norris *et al.*, 2000). The result is a nonwoven fibrous scaffold with a high surface-area-to-volume ratio and small pores (in microns). Many factors influence fiber thickness and morphology, including solution qualities (viscosity, elasticity, conductivity, and surface tension), electric field strength, the distance between the spinneret and the collecting plate, temperature, and humidity (Jose Varghese *et al.*, 2019).

There are two types of electrospinning configurations now available: vertical and horizontal. Several research groups have created more sophisticated technologies that can fabricate more complicated nanofibrous structures in a more regulated and efficient manner as this technology has advanced (Kidoaki, Kwon and Matsuda, 2005; Stankus *et al.*, 2006).

Research objectives

The proposed research is set out to achieve the following specific objectives:

1) Polymerization of methyl vinyl ketone.
2) Evaluation of reaction conditions for synthesizing variable molecular weight poly (methyl vinyl ketone).
3) Synthesis of poly (3-buten-2-ol) by reducing the poly (methyl vinyl ketone) synthesized.
4) Evaluation and characterization (FTIR, NMR, GPC, DSC, TGA) of synthesized polymers.
5) Exploring the possibility of processing the polymers into fibers and nanoparticles.
6) Evaluation of potential application in hydrogen storage.

CHAPTER III

METHODOLOGY

Chemicals

- 2,2'-Azobis(2-methylpropionitrile) 98% by Sigma-Aldrich
- Methyl vinyl ketone, tech. 90%, stab. by Alfa Aesar
- Sodium borohydride 98+%, powder by Acros Organics
- Ethyl alcohol, anhydrous, 200 Proof, 99.5+% by Acros Organics
- Tetrahydrofuran, anhydrous, 99.8%, BHT-free by Alfa Aesar
- Methanol, laboratory-grade by Fisher Chemicals.
- *n*-Heptane for HPLC (approx., 99% *n*-heptane) by Fisher Chemicals.

Synthesis

Polymerization

Polymerization of methyl vinyl ketone was done using a modified method from Oka et al (2021). Under argon, 2,2′-azobis(isobutyronitrile) (AIBN) was dissolved in methyl vinyl ketone, after which the solution was heated to 70°C and stirred for 3 hours. The monomers were then removed from the polymer precipitate, leaving a yellowish solid (Oka *et al.*, 2021). The polymer was then cleaned by dissolving in THF and reprecipitating in *n*-heptane in a 1:2 ratio, followed by evaporation. You do not tell me the grams of monomer and AIBN used, even if you present a table underneath, you should say "A typical synthesis procedure involved 0.8 ml of methyl vinyl ketone, 0.017 g of AIBN), heated to 70 °C and stirred for 3 hours.

Preparation of poly (3-buten-2-ol)

THF/ethanol (4/3)-mixed solvents were used to dissolve poly(methyl vinyl ketone) (0.42 g, 6.0 mmol). A total of 60 mmol sodium borohydride was then added. For 24 hours, the solution was agitated. After that, the precipitate was dissolved in methanol and reprecipitated with THF to produce a white powder (Oka *et al.*, 2021).

Characterization

Polymers formed were analyzed using a combination of techniques. These techniques included Nuclear Magnetic Resonance (NMR), Fourier Transform Infrared spectroscopy (FTIR), Differential Scanning Calorimetry (DSC), Gel Permeation Chromatography (GPC), and Thermogravimetric Analysis (TGA).

Fourier Transform Infrared (FTIR) Spectrophotometer

Infrared Spectroscopy was done with a Bruker vertex 70 FT-IR spectrometer with single reflection diamond ATR and OPUS software with the resolution set to 4 cm^{-1}, scans set to 256, and background scans set to 256. The frequency range used was 4000–400 cm^{-1}.

Differential scanning calorimeter

NETZSCH DSC 214 polymer analyzer with inbuilt temperature range of -170°C–600°C was used to obtain DSC thermograms. 10 mg of the sample was placed in the apparatus and heated at

a rate of 10.0 °C min^{-1} from 0 to 270 °C in a nitrogen environment. The results were exported and plotted in OriginPro.

Thermogravimetric analyzer

The NETZSCH TG 209 F3 Tarsus analyzer was used to acquire TGA thermograms. The studies were carried out using a tiny amount of sample (10 mg) heated at a rate of 10 °C min^{-1} from 27 °C to 700 °C in a nitrogen environment. The results were exported and plotted in OriginPro.

Gel Permeation Chromatography

The samples were characterized by Gel Permeation Chromatography (GPC) with conventional calibration (Polystyrene standards). Multi Angle Light Scattering (GPC-MALS) was also used. Because the concentration dependence of the index of refraction (dn/dc) of the samples is not known, all calculations were only done using conventional calibration.
All samples were prepared at a concentration of 5–7 mg ml^{-1} in tetrahydrofuran (THF) and filtered through a 0.2 µm PTFE syringe filter. The separations were carried out using an EcoSEC Elite GPC System (Tosoh Bioscience LLC, King of Prussia, PA). A guard column (5 µm, 50x7.8 mm^2) and two Phenogel 300 x 7.8 mm columns (Phenomenex, Torrance, CA), connected in series: (1) 5 µm, 104Å (5–1800 K); (2) 5 µm, Linear(2)(100–10,000 K) were used for the separation.
For detection, the EcoSEC differential refractive index detector, or a Lens3 multiangle light scattering detector (also from Tosoh) with a 20 mW, 505 nm Diode Laser were used. All

separations were done using an injection volume of 100µL. THF stabilized with 250 ppm of BHT (1 ml min^{-1}) was used as the solvent. Data acquisition and data processing were performed using the SEC view Software from Tosoh. The data was then analyzed with the help of Microsoft Excel and OriginPro.

Nuclear Magnetic Resonance

Nuclear Magnetic Resonance was performed using a Bruker FT-NMR at 600 MHz with Kimble borosilicate glass N-51A 5mm NMR tubes. The chemical shift range was set to be between 0 and 10 ppm, and the number of scans was set at 16. Deuterated chloroform ($CDCl_3$) was the solvent.

Processing polymer

Electrospinning

Electrospinning was conducted on the polymer via solution electrospinning with THF as the solvent and with varied concentration and separation distance. Figure 3. 1 shows PMVK fibers being extruded from the needle tip. The parameters that yielded the fiber were: concentration of 25% m v^{-1} , voltage of 25 kV, flow rate of 0.01 ml min^{-1} and separation of 21 cm at ambient temperature.

Figure 3. 1: Fiber extruded from needle tip

CHAPTER IV

RESULTS AND DISCUSSION

The synthesis involved the free radical polymerization of the methyl vinyl ketone monomer, which was initiated by AIBN. Figure 4. 1 shows the overall sequence of polymerization and Figure 4. 2 shows the overall reaction scheme.

Drying purging reaction polymer

Figure 4. 1: Polymerization of methyl vinyl ketone

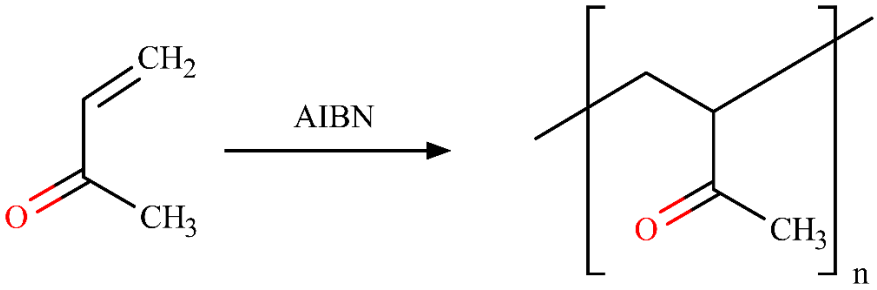

Figure 4. 2: Chemical equation for the polymerization of methyl vinyl ketone with AIBN

After an hour, the stirring action of the magnetic stirring bar began to slow down as the solution increased its viscosity (use chemical terms) . The stirring almost came to a stop after 2.5 hours as the content of the flask became very viscous. It was observed that the color of the solution became dark yellow as the products were being formed and became darker still after drying. The final product had a gooey consistency and hardly flowed at room temperature but began to flow at elevated temperatures.

Figure 4. 3: Gooey consistency demonstrated using tweezers to pull the polymer

The mole percent concentration of the initiator (AIBN) was varied to produce different conversion rate of the polymer as shown in Table 4. 1.

Table 4. 1: Difference in yield due to variation in initiator concentration

AIBN (mole%)	Mass of AIBN (g)	Volume of MVK (ml)	Mass of PMVK (g)	Conversion %
0.1	**0.017**	**0.8**	**0.3288**	**48.93**
0.2	**0.033**	**0.8**	**0.4015**	**59.75**
0.5	**0.084**	**0.8**	**0.4476**	**66.61**
1.0	**0.167**	**0.8**	**0.5125**	**76.26**
2.0	**0.333**	**0.8**	**0.5335**	**79.39**

The polymer was soluble in THF, chloroform, acetone, and methanol. It was also realized on visual inspection that the polymers produced with different amounts of AIBN resulted in polymers with slight color differences: The polymer produced with the least amount of initiator has a yellowish color which changes gradually toward orange as the concentration of initiator increases, as shown in figure 4. 4.

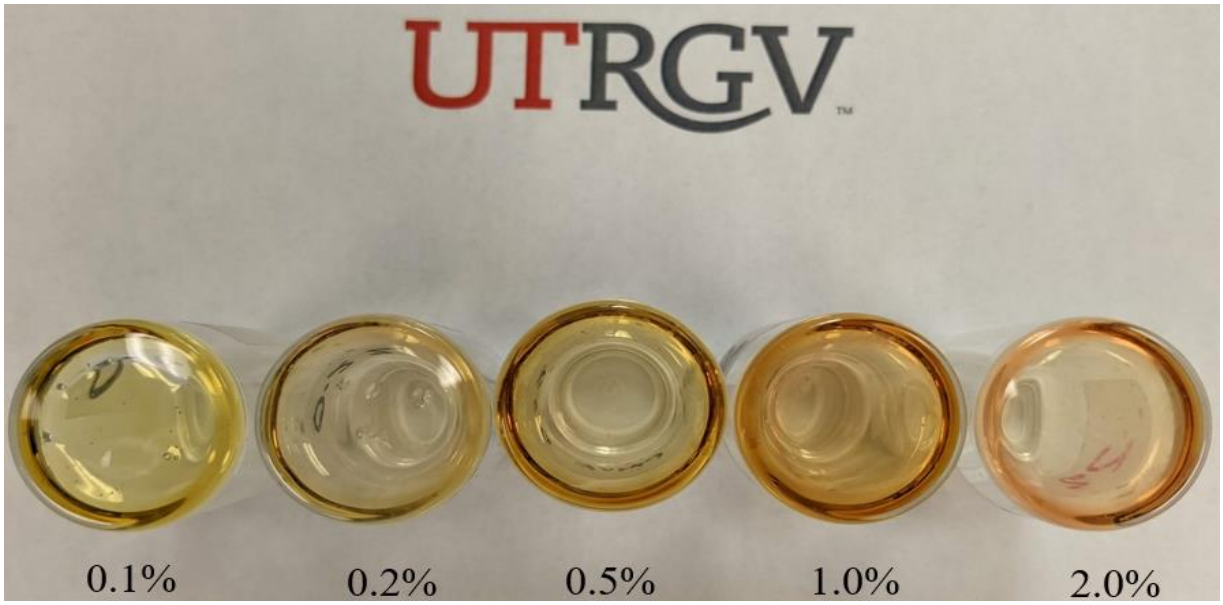

Figure 4. 4: Variation in color with as concentration on AIBN is varied

The polymer with the lowest initiator concentration was cleaned by further dissolving in THF and reprecipitating with *n*-heptane, followed by and evaporation of the solvents; this was done once (1C), twice (2C), and 5 times (5C). After every cycle, the color of the polymer changed from a bright yellow to a paler yellow as shown in figure 4. 5, suggesting that the hydroquinone inhibitor was being removed after each cleaning cycle

Figure 4. 5: Color variation after cleaning; from left to right: original sample, 1 cycle of cleaning, 2 cycles of cleaning, and 5 cycles of cleaning.

Poly (3-buten-2-ol) was synthesized by reducing poly (methyl vinyl ketone) with sodium borohydride to yield a white precipitate as shown in figure 4.7.

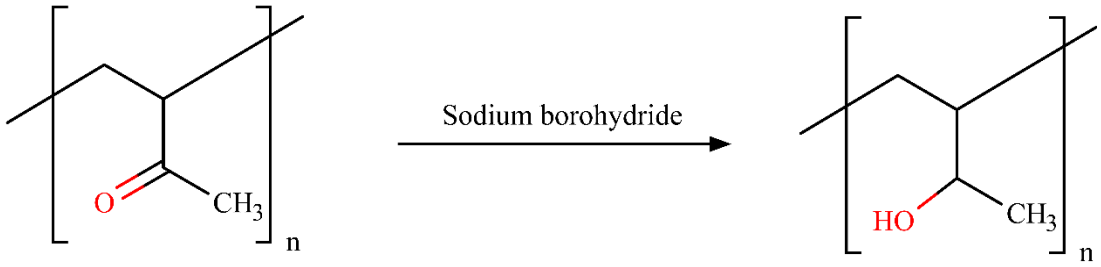

Figure 4. 6: Chemical equation for the reduction of PMVK to poly (3-buten-2-ol)

Figure 4. 7: Reduction of poly (methyl vinyl ketone) to form poly (3-buten-2-ol)

A reflux set-up with a drying tube affixed on top was employed to prevent excessive absorption of moisture by the sodium borohydride–polymer mixture, because sodium borohydride is highly hygroscopic. During the reduction, it was observed that the yellowish coloration of the solution gradually faded to a white color after 20 hrs. The final product was a white precipitate in the mixture that settles when allowed to stand. The product was filtered under vacuum, after which the residue was dissolved in methanol and reprecipitated in THF in a 1:2 ratio to ensure maximum reprecipitation. The clear solution was then gently poured off and the precipitate was dried to yield a white powder as shown below in figure 4.8.

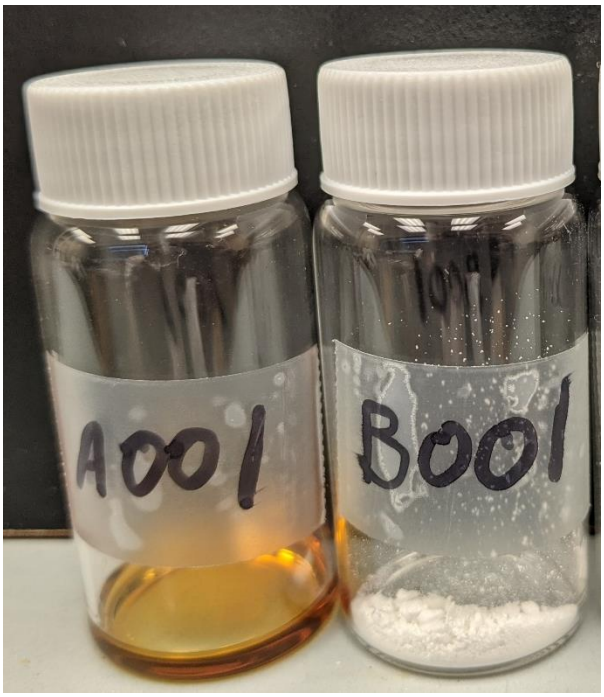

Figure 4. 8: PMVK (left) compared to poly (3-buten-2-ol)

Characterization of poly (methyl vinyl ketone)

The sample produced was found to be soluble in THF, methanol, chloroform, acetone, and acetic acid. FTIR analysis using the Bruker Vertex 70 FT-IR spectrometer, showed peaks around 2940 cm^{-1}, which corresponds to C-H stretching, and 1705 cm^{-1}, which corresponds to C=O stretching. Moisture absorbance was also detected as a characteristic feature at 3500 cm^{-1}. This was observed for both the cleaned and uncleaned samples, but the intensity of the peaks decreased significantly with PMVK 5C; there was also a slight difference in the fingerprint region around 1000 cm^{-1}, as shown in Fig. 4. 9. The reduction in peak height after cleaning may be due to the fact that the PMVK 5C was more crystalline and less tightly packed than the others, such that the infrared radiation did not as probe many molecules per unit area. The difference in

the fingerprint region may be due to a reduction in the number of low molecular weight polymers in the sample or the presence of the precipitating agent.

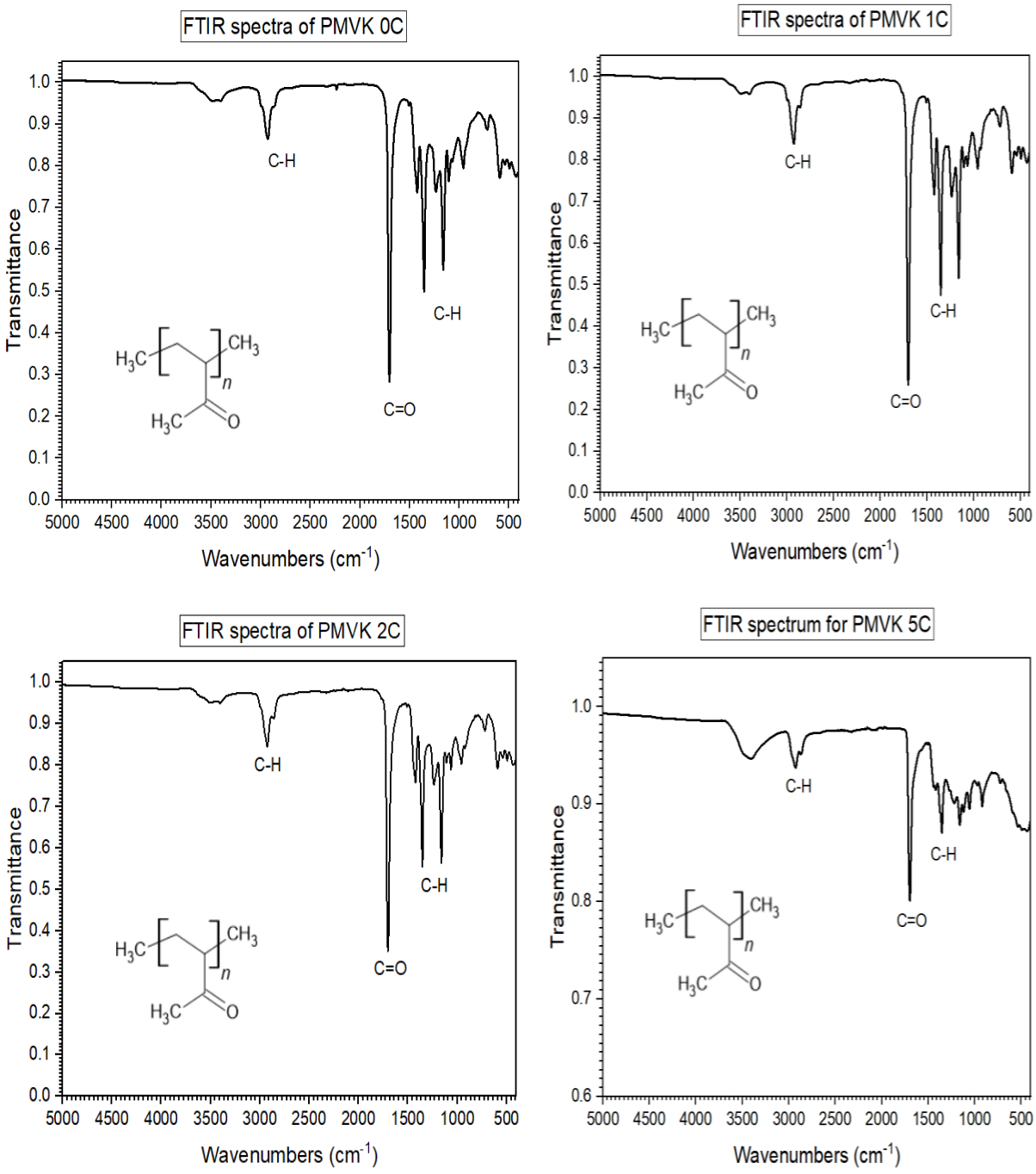

Figure 4. 9: FTIR spectra of PMVK

The FTIR spectrum of poly(methyl vinyl ketone) is generally similar to that of methyl vinyl ketone, as shown in figure 4. 10, with the principal differences being in the carbon-to-carbon double bond region (~1700 cm^{-1}) and the fingerprint region (<1400 cm^{-1}). The carbon-to-carbon double bond that appears in the MVK spectra is noticeably absent in the PMVK spectra which is an indication of the conversion of the carbon-to-carbon double bond to single bonds. The carbon-to-oxygen double bond peak that was detected at 1680 cm^{-1}, corresponding to a conjugated ketone, in the methyl vinyl ketone shifted to a carbon-to-oxygen double bond peak at 1705 cm^{-1}, corresponding to an aliphatic ketone in the poly(methyl vinyl ketone).

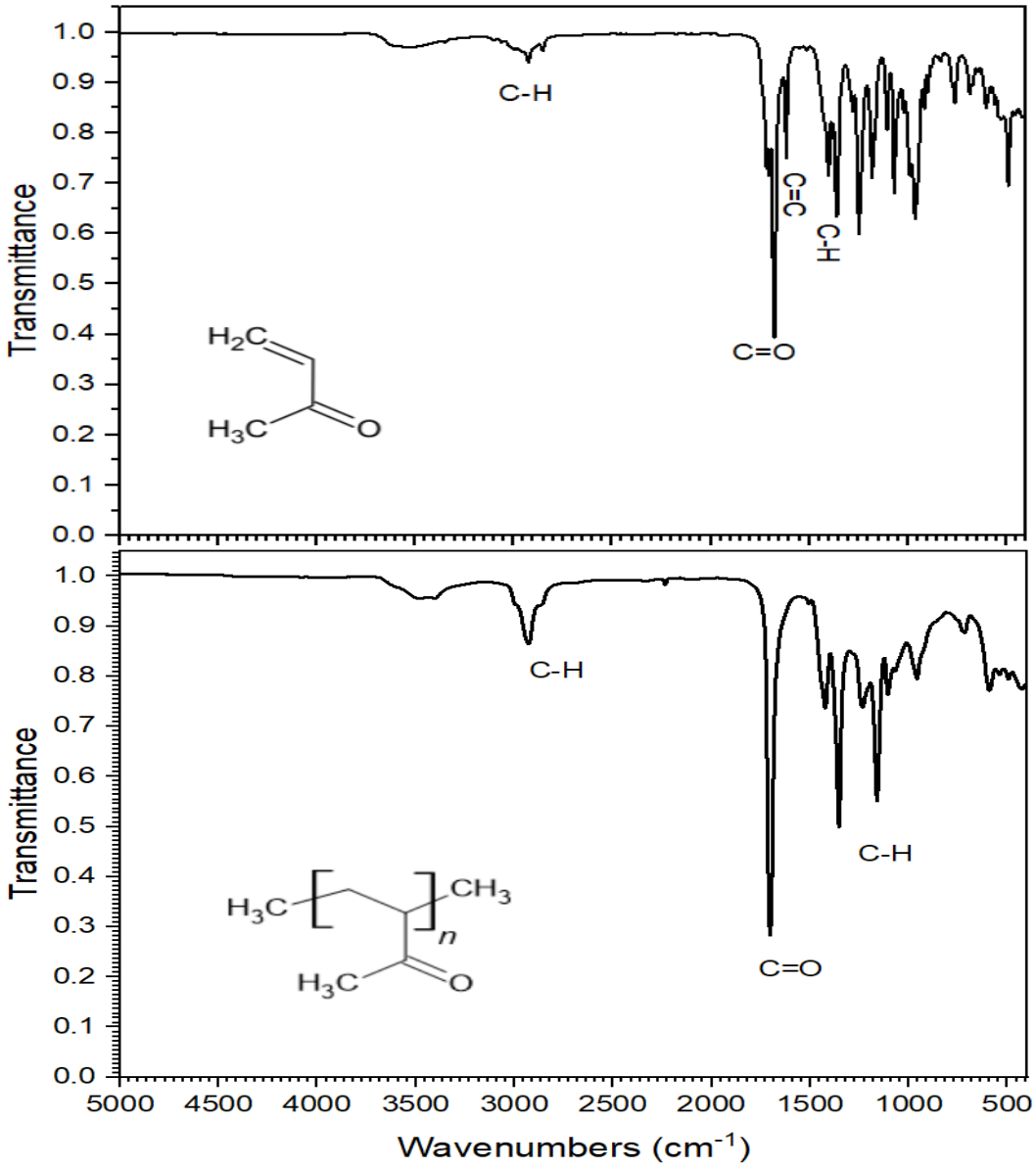

Figure 4. 10: FTIR spectra of MVK (top) compared with FTIR spectra of PMVK(bottom)

Thermogravimetric analysis was also carried out on the samples to assess the degradation behavior of the sample using a NETZSCH TG 209F3 thermogravimetric analyzer with a 10 K/min heating rate. PMVK underwent 3% weight loss at 120 ^{o}C which might be due to loss of moisture. There are signs of degradation around 150 ^{o}C.

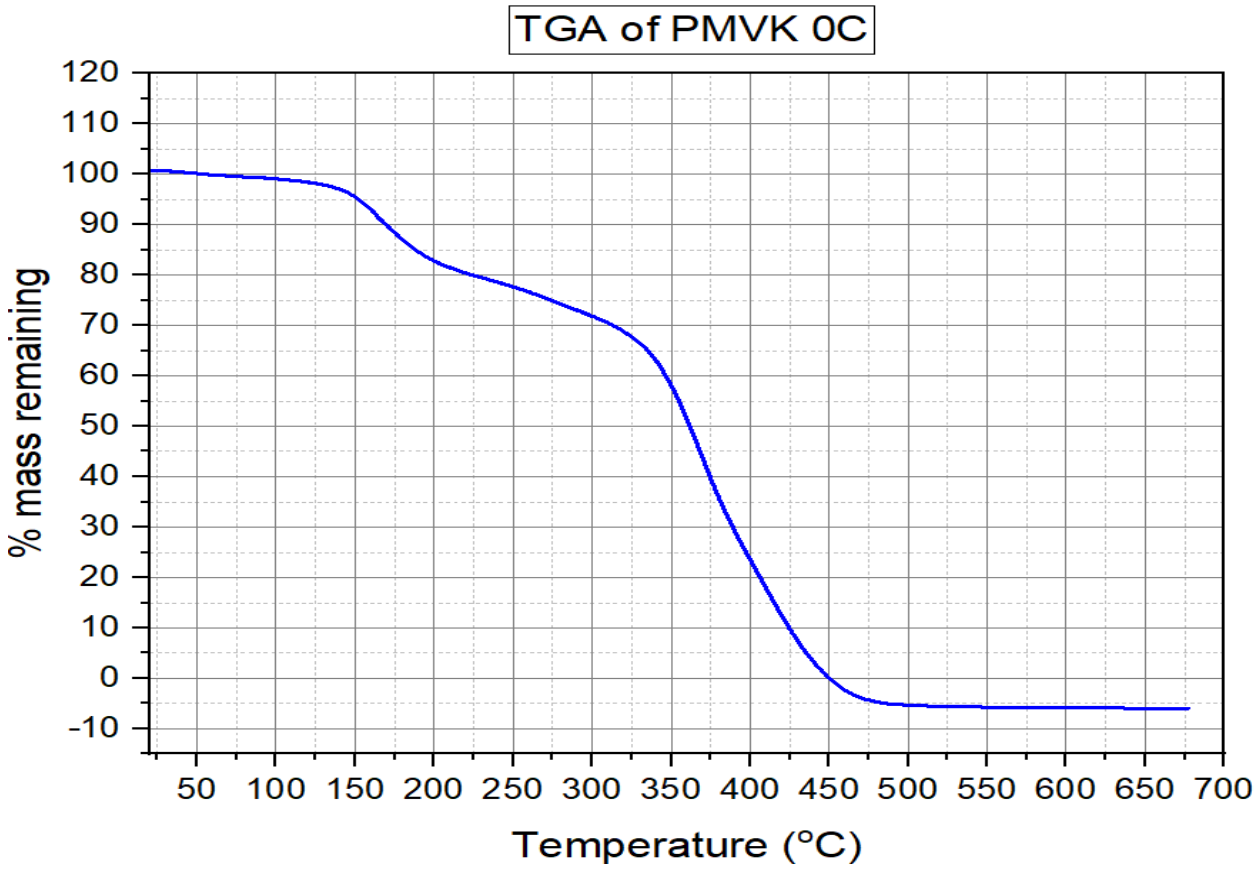

Figure 4. 11: Thermogravimetry behavior of PMVK

Differential scanning calorimetry was also conducted using the NETZSCH DSC 214, as presented in Fig. 4. 12. The glass transition temperature of PMVK was found to be ~3.5 ^{o}C. The DSC graph also shows a peak around 150 ^{o}C, which is indicative of degradation (as corroborated by the thermogravimetric data).

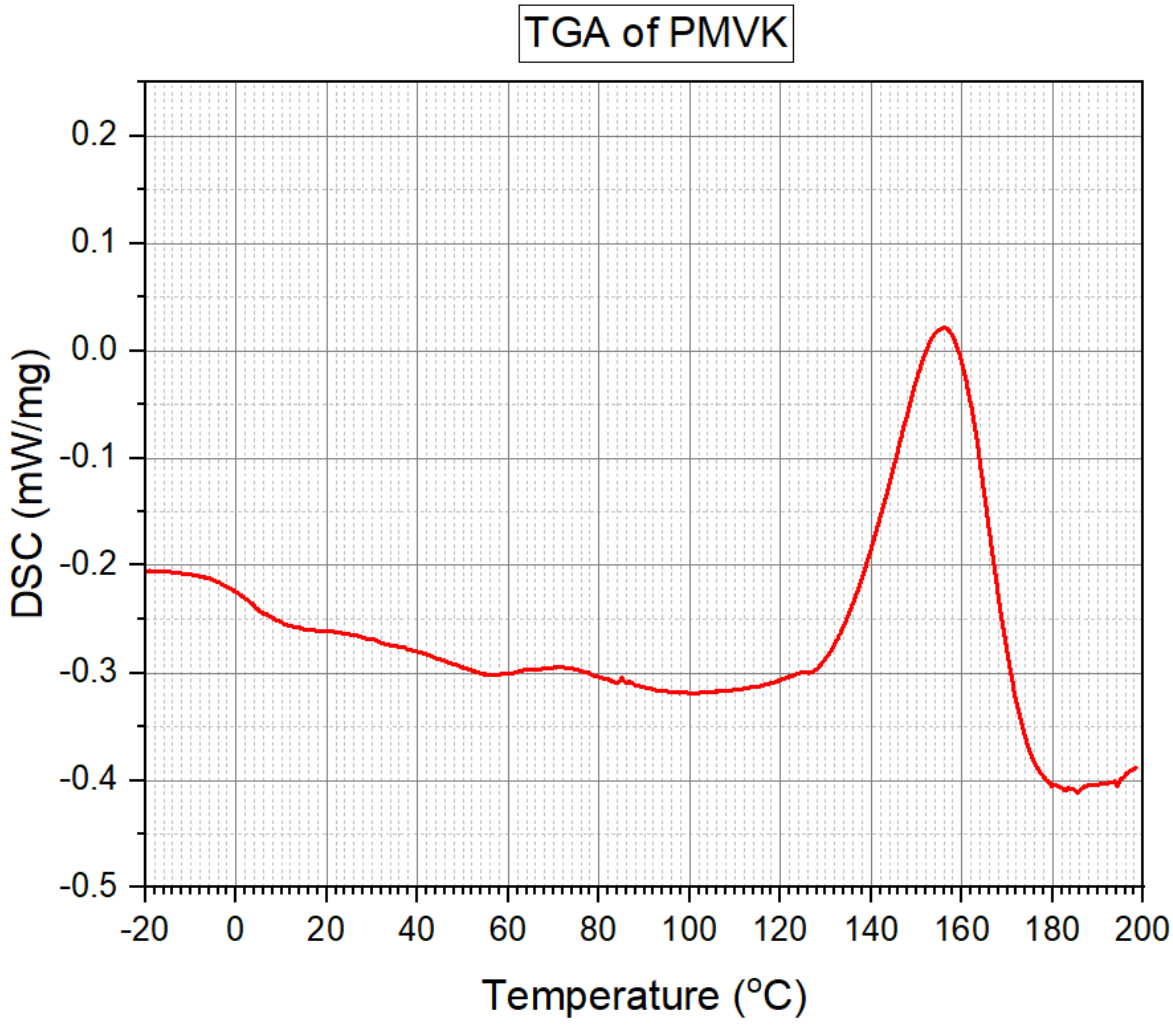

Figure 4. 12: DSC curve of PMVK

Nuclear Magnetic Resonance spectroscopy (NMR) conducted on the PMVK (shown in Figure 4.13) indicates that the samples obtained were not pristine. Numerous contaminant features appear in the spectrum as compared with a literature reference.

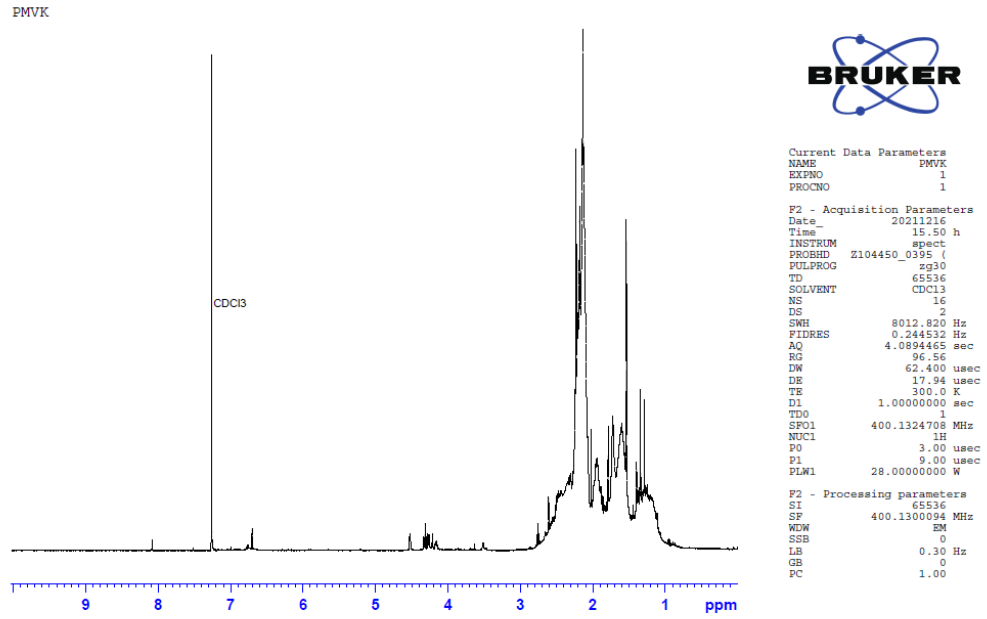

Figure 4. 13: NMR spectrum of PMVK

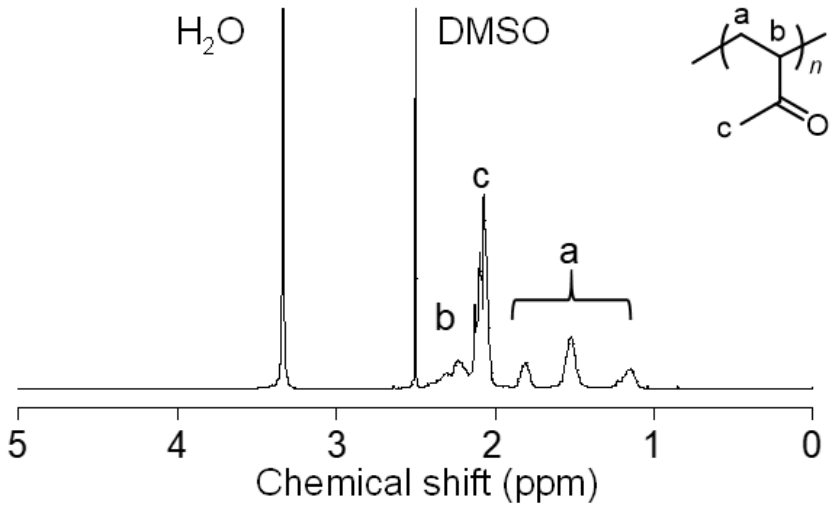

Figure 4. 14: NMR spectrum from literature

(Oka *et al.*, 2021)

Gel Permeation Chromatography

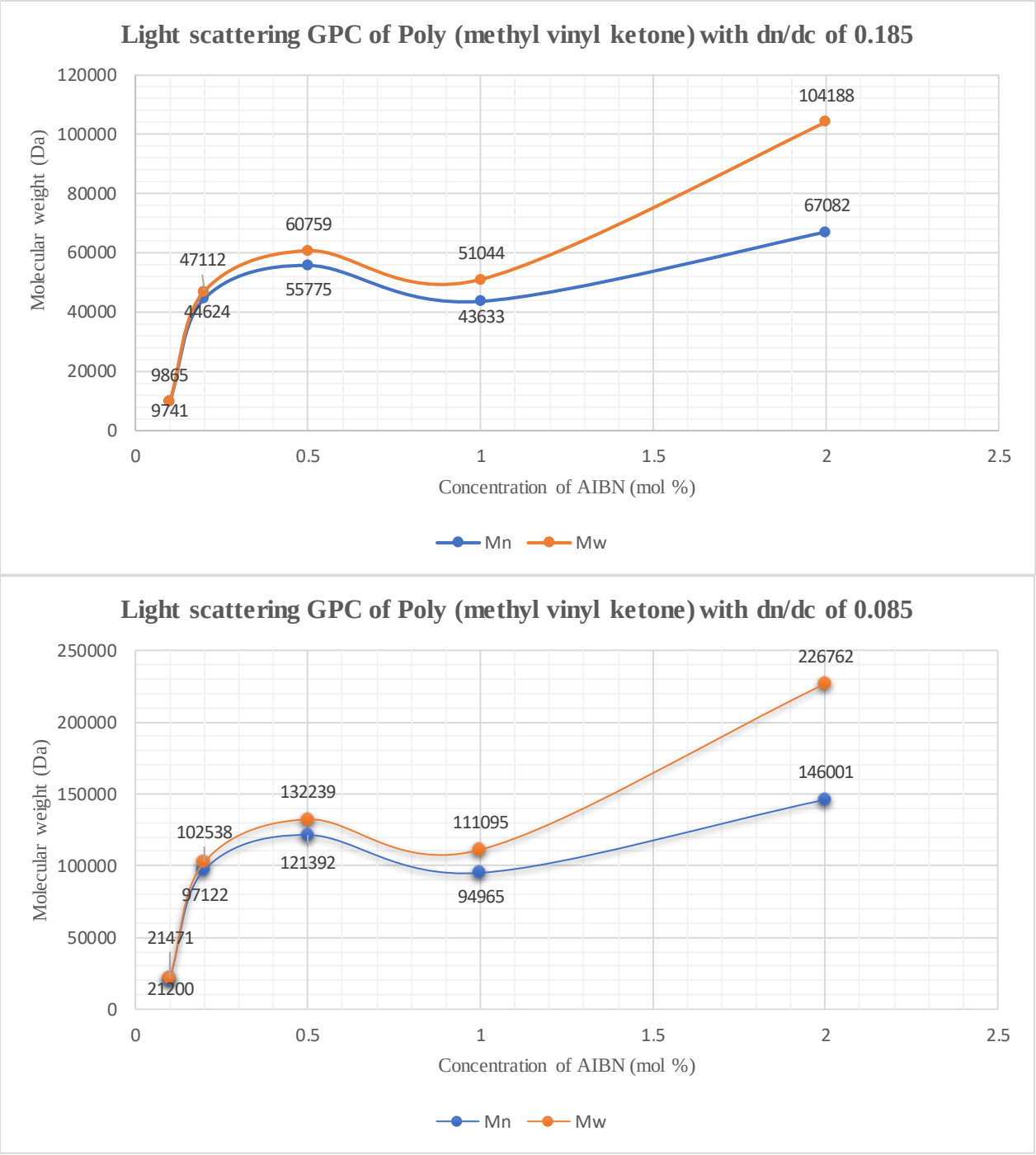

Figure 4. 15: Graph of molecular weight against AIBN concentration of PMVK

Gel permeation chromatography using a light scattering (LS) detector shows a general increase in molecular weight as concentration of AIBN increased. The LS using dn/dc of 0.185 recorded lower molecular weight averages as compared of to the LS using dn/dc of 0.085. Both, however, show a similar trend in molecular weight averages with the exactly the same polydispersity index (Mn/Mw) of 1.013, 1.056, 1.089, 1.17 and 1.553 for 0.1%, 0.2%, 0.5%, 1% and 2% AIBN, respectively. The molecular weight trend does not follow the typical pattern of molecular weight with varying concentrations of initiator. This may be due to the presence of hydroquinone, which was used to inhibit the spontaneous polymerization of the MVK purchased. The hydroquinone was not removed prior to synthesis, as it was thought that it would be consumed completely with higher amounts of AIBN, which could be impeding the achievement of higher molecular weight with lower concentration of the initiator.

Characterization of Poly (3-buten-2-ol)

The poly (3-buten-2-ol) synthesized was whitish powder and found to be soluble in water, methanol acetic acid and ethylene glycol but insoluble in ethanol, isopropanol, butanol, dimethyl sulfoxide (DMSO), THF, and chloroform, even after heating.

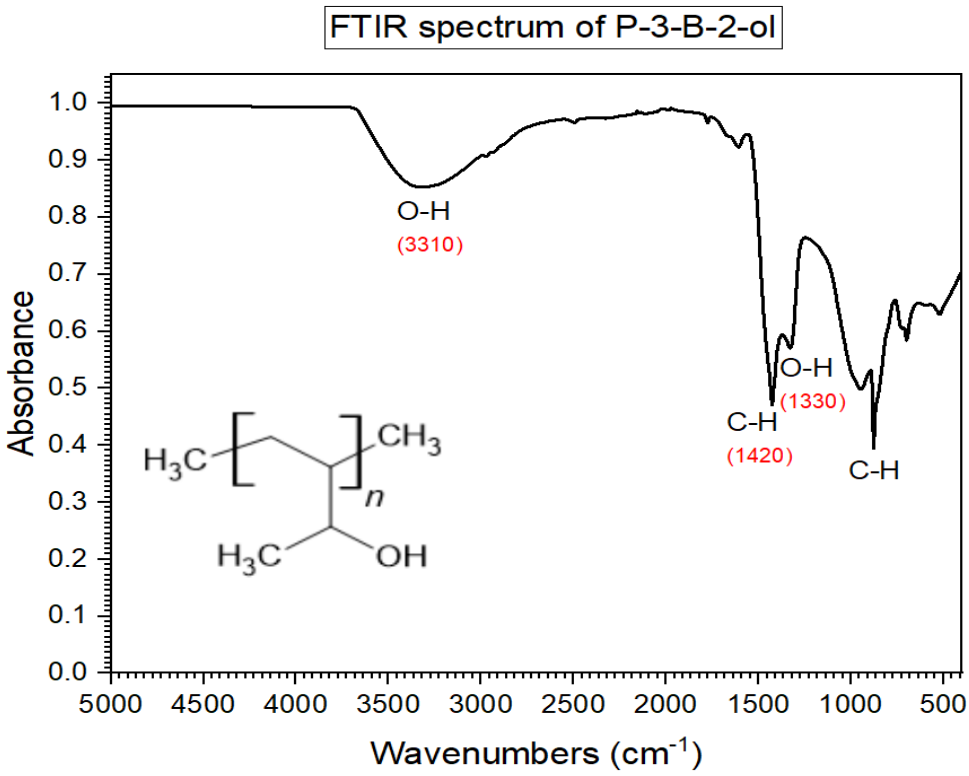

Figure 4. 16: FTIR spectra of poly (3-buten-2-ol)

FTIR analysis using the Bruker vertex 70 FT-IR spectrometer, showed the peaks around: 3310 and 1330 cm^{-1} for OH stretching and bending, and 1420 cm^{-1}, which corresponds to C-H stretching.

Processing of Poly (methyl vinyl ketone)

Figure 4. 17: Electrospun fibers of PMVK

Initial electrospinning attempts yielded fibers, as shown in figure 4. 17, but when the fibers were left standing in air for about 30 minutes, they absorbed atmospheric moisture and started

forming films, as can be seen in Figure 4.18. This hydrophilicity could be reduced with higher molecular weight polymers.

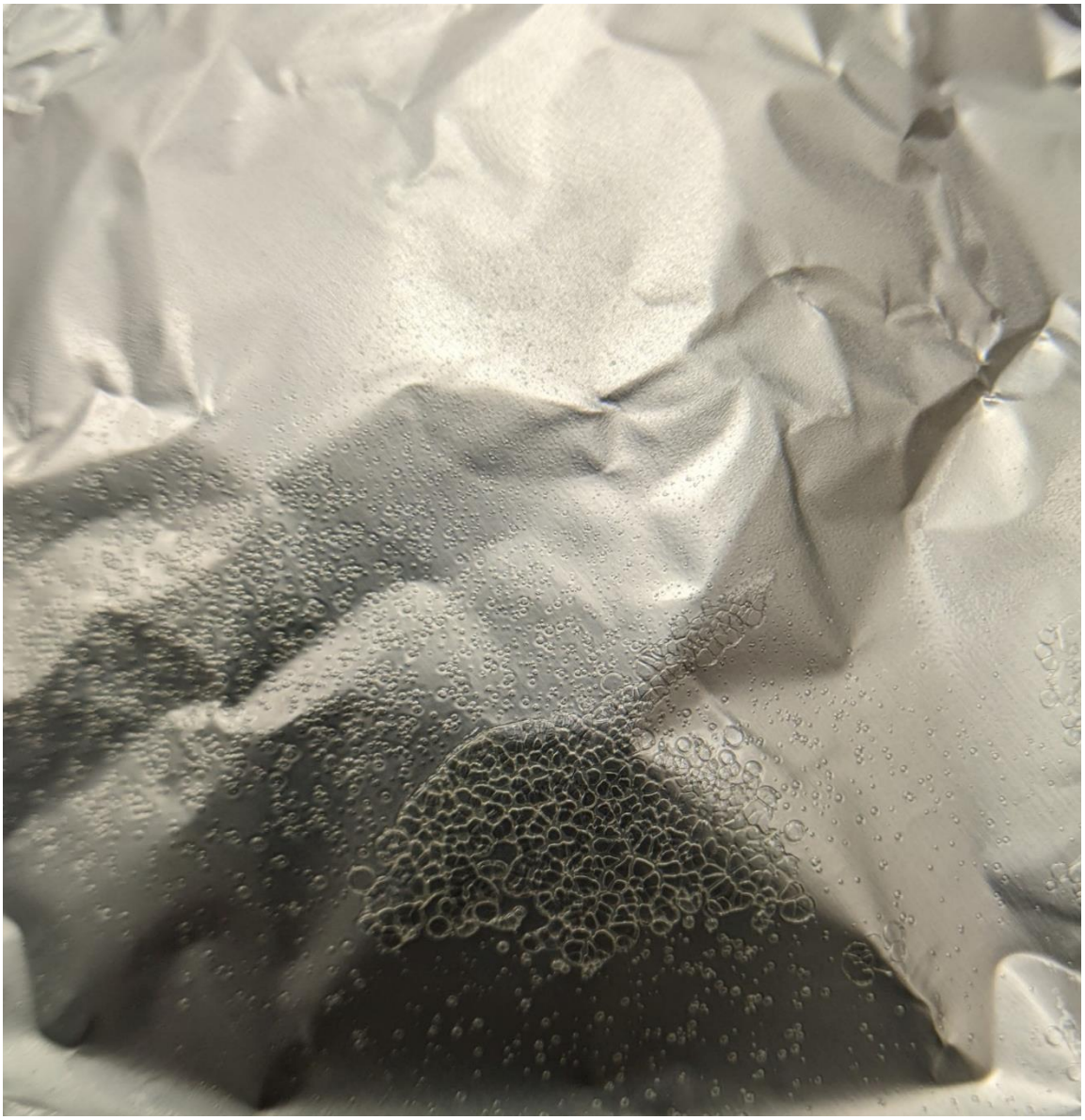

Figure 4. 18: PMVK films

CHAPTER V

CONCLUSION

Poly (methyl vinyl ketone) was successfully synthesized and the effect of initiator concentration on the conversion rate and molecular weight of the polymer were explored. The initiator concentration was found to be directly proportional to the conversion rate and molecular weight of the polymer produced with the help of gel permeation chromatography, with higher concentration of initiator producing higher conversion rate and higher molecular weight polymers. The apparent deviation of the molecular weight trend from expectations could be attributed to the presence of a hydroquinone inhibitor in the methyl vinyl ketone monomer. Poly (methyl vinyl ketone) was also successfully reduced to poly (3-buten-2-ol) using sodium borohydride. Characterization confirmed the formation of poly (methyl vinyl ketone) and poly(3-buten-2-ol). The poly (methyl vinyl ketone) was electrospun with some success, but the resulting fibers readily absorbed moisture to become films. Work is underway to remove the hydroquinone stabilizer in the monomer before polymerization is carried out. The polymerization will then be optimized, and fiber and nanoparticle synthesis will be explored further.

REFERENCES

Abdalla, A. M. *et al*. (2018) 'Hydrogen production, storage, transportation and key challenges with applications: A review', *Energy Conversion and Management*, 165(January), pp. 602–627. doi: 10.1016/j.enconman.2018.03.088.

Ahn, Y. C. *et al*. (2006) 'Development of high efficiency nanofilters made of nanofibers', *Current Applied Physics*, 6(6 SPEC. ISS.), pp. 1030–1035. doi: 10.1016/j.cap.2005.07.013.

Aiello, R. *et al*. (1998) 'Production of hydrogen gas from novel chemical hydrides', *International Journal of Hydrogen Energy*, 23(12), pp. 1103–1108. doi: 10.1016/S0360-3199(98)00001-9.

Andersson, J. and Grönkvist, S. (2019) 'Large-scale storage of hydrogen', *International Journal of Hydrogen Energy*, 44(23), pp. 11901–11919. doi: 10.1016/j.ijhydene.2019.03.063.

Balat, M. (2008) 'Potential importance of hydrogen as a future solution to environmental and transportation problems', *International Journal of Hydrogen Energy*, 33(15), pp. 4013–4029. doi: 10.1016/j.ijhydene.2008.05.047.

Barilo, N. and Suzanne, L. (2018) 'Hydrogen Fuel Cells and the Fuel Cell Electric Vehhicles: Emerging Applications and Safety Management', in *Green Transportation Summit & Expo*.

Bellosta von Colbe, J. *et al*. (2019) 'Application of hydrides in hydrogen storage and compression: Achievements, outlook and perspectives', *International Journal of Hydrogen Energy*, 44(15), pp. 7780–7808. doi: 10.1016/j.ijhydene.2019.01.104.

Bénard, P. and Chahine, R. (2007) 'Storage of hydrogen by physisorption on carbon and nanostructured materials', *Scripta Materialia*, 56(10), pp. 803–808. doi: 10.1016/j.scriptamat.2007.01.008.

Braun, D. (2009) 'Origins and Development of Initiation of Free Radical Polymerization Processes', *International journal of polymer science*, 2009(April 1863). doi: 10.1155/2009/893234.

Buijs, H. (2006) 'Infrared Spectroscopy', *Springer Handbooks*, 71(12), pp. 607–613. doi: 10.1007/978-0-387-26308-3_40.

Carraher Jr., C. E. (2011) *Carraher's Polymer Chemistry*. 8th edn. CRC Press. Available at: https://www.google.com/search?source=hp&ei=nyf-XKDKB-rez7sP6OSe8As&q=carraher%27s+polymer+chemistry+eighth+edition+pdf&oq=&gs_l=psy-ab.1.0.35i39l6.0.0..3632...1.0..0.106.106.0j1.....0.....gws-wiz.....6.5dNsjAawDr8.

Chang, Q. (2016) *Surface of Solids*. doi: 10.1016/B978-0-12-809315-3/00010-4.

Chen, X. *et al*. (2021) 'Li-fluorine codoped electrospun carbon nanofibers for enhanced hydrogen storage', *RSC Advances*, 11(7), pp. 4053–4061. doi: 10.1039/d0ra06500e.

Clayden, J., Greeves, N. and Warren, S. (2012) *Organic Chemistry*. Oxford University Press. doi: 10.1016/b978-0-12-676950-0.50001-8.

Crabtree, G. W. and Dresselhaus, M. S. (2008) 'The hydrogen fuel alternative', *MRS Bulletin*, 33(4), pp. 421–428. doi: 10.1557/mrs2008.84.

Davis, F. J. (ed.) (2005) *Practical approach in chemistry series: Polymer Chemistry*. Oxford University Press.

Ding, F. and Yakobson, B. I. (2015) 'Challenges in hydrogen adsorptions : from physisorption to chemisorption', 6(2), pp. 142–150. doi: 10.1007/s11467-011-0171-6.

Dunn, S. (2002) 'Hydrogen futures: Toward a sustainable energy system', *International Journal of Hydrogen Energy*, 27(3), pp. 235–264. doi: 10.1016/S0360-3199(01)00131-8.

Ebnesajjad, S. (2011) *Surface and material characterization techniques, Handbook of Adhesives and Surface Preparation*. Elsevier Inc. doi: 10.1016/B978-1-4377-4461-3.10004-5.

Environ, E. *et al*. (2012) 'Environmental Science Assessment of hydrogen storage by physisorption in porous materials', pp. 8294–8303. doi: 10.1039/c2ee22037g.

Flory, P. J. (1937) 'The Mechanism of Vinyl Polymerizations', *Journal of the American Chemical Society*, 59(2), pp. 241–253. doi: 10.1021/ja01281a007.

Gellerstedt, G. (1992) 'Gel Permeation Chromatography', in *Methods in Lignin Chemistry*. Springer, pp. 487–497. Available at: https://link.springer.com/chapter/10.1007/978-3-642-74065-7_34?noAccess=true.

Graetz, J. (2009) 'New approaches to hydrogen storage', *Chemical Society Reviews*, 38(1), pp. 73–82. doi: 10.1039/b718842k.

Grimes, C. A., Varghese, O. K. and Ranjan, S. (2008) *Light, Water, Hydrogen: The Solar Generation of Hydrogen by Water Photoelectrolysis, Springer*. doi: 10.1021/ja803884k.

Hirscher, M., Panella, B. and Schmitz, B. (2010) 'Microporous and Mesoporous Materials Metal-organic frameworks for hydrogen storage', *Microporous and Mesoporous Materials*, 129(3), pp. 335–339. doi: 10.1016/j.micromeso.2009.06.005.

Huang, Z. M. *et al*. (2003) 'A review on polymer nanofibers by electrospinning and their applications in nanocomposites', *Composites Science and Technology*, 63(15), pp. 2223–2253. doi: 10.1016/S0266-3538(03)00178-7.

Inan, T. Y. (2017) *Thermoplastic-based nanoblends: Preparation and characterizations*, *Recent Developments in Polymer Macro, Micro and Nano Blends: Preparation and Characterisation*. Elsevier Ltd. doi: 10.1016/B978-0-08-100408-1.00002-9.

Jose Varghese, R. *et al.* (2019) *Introduction to nanomaterials: Synthesis and applications*, *Nanomaterials for Solar Cell Applications*. Elsevier Inc. doi: 10.1016/B978-0-12-813337-8.00003-5.

Kato, R. *et al.* (2016) 'A ketone/alcohol polymer for cycle of electrolytic hydrogen-fixing with water and releasing under mild conditions', *Nature Communications*, 7, pp. 1–7. doi: 10.1038/ncomms13032.

Kato, R. and Nishide, H. (2018) 'Polymers for carrying and storing hydrogen', *Polymer Journal*, 50(1), pp. 77–82. doi: 10.1038/pj.2017.70.

Kidoaki, S., Kwon, I. K. and Matsuda, T. (2005) 'Mesoscopic spatial designs of nano- and microfiber meshes for tissue-engineering matrix and scaffold based on newly devised multilayering and mixing electrospinning techniques', *Biomaterials*, 26(1), pp. 37–46. doi: 10.1016/j.biomaterials.2004.01.063.

Lannutti, J. *et al.* (2007) 'Electrospinning for tissue engineering scaffolds', *Materials Science and Engineering C*, 27(3), pp. 504–509. doi: 10.1016/j.msec.2006.05.019.

Larranaga, M. D., Lewis, R. J. S. and Lewis, R. A. (2016) *Hawley's Condensed Chemical Dictionary*. 16th edn, *American Journal of Therapeutics*. 16th edn. John Wiley and Sons.

Lee, K. J. *et al.* (2013) 'Feasibility of compression ignition for hydrogen fueled engine with neat hydrogen-air pre-mixture by using high compression', *International Journal of Hydrogen Energy*, 38(1), pp. 255–264. doi: 10.1016/j.ijhydene.2012.10.021.

Levesque, C. L. (1982) 'The Structure of Vinyl Polymers : the Polymer from Methyl Vinyl Ketone', *contributions from the research laboratory of organic chemistry, Massachusetts institute of technology*, 60(2), pp. 280–284. Available at: https://pubs.acs.org/doi/pdf/10.1021/ja01269a016.

Li, G. *et al.* (2014) 'Hydrogen storage in Pd nanocrystals covered with a metal-organic framework', *Nature Materials*, 13(8), pp. 802–806. doi: 10.1038/nmat4030.

Liang, D., Hsiao, B. S. and Chu, B. (2007) 'Functional electrospun nanofibrous scaffolds for biomedical applications', *Advanced Drug Delivery Reviews*, 59(14), pp. 1392–1412. doi: 10.1016/j.addr.2007.04.021.

Lototskyy, M. V. *et al.* (2015) 'Metal hydride systems for hydrogen storage and supply for stationary and automotive low temperature PEM fuel cell power modules', *International Journal of Hydrogen Energy*, 40(35), pp. 11491–11497. doi: 10.1016/j.ijhydene.2015.01.095.

Lysak, D. H., Simpson, M. J. and Simpson, A. J. (2022) *Applications of nuclear magnetic resonance for the study of soils*. 2nd edn, *Reference Module in Earth Systems and Environmental Sciences*. 2nd edn. Elsevier Ltd. doi: 10.1016/b978-0-12-822974-3.00021-5.

Ma, L. J. *et al.* (2020) 'Cooperative physisorption and chemisorption of hydrogen on vanadium-decorated benzene', *RSC Advances*, 10(62), pp. 37770–37778. doi: 10.1039/d0ra06057g.

Mahato, N. *et al.* (2020) *Recent progress in conducting polymers for hydrogen storage and fuel cell applications*, *Polymers*. doi: 10.3390/polym12112480.

Malvern Instruments Worldwide (2013) 'White paper: Static Light Scattering technologies for GPC/SEC explained', pp. 1–28.

Marchenko, O. V. and Solomin, S. V. (2015) 'The future energy: Hydrogen versus electricity', *International Journal of Hydrogen Energy*, 40(10), pp. 3801–3805. doi: 10.1016/j.ijhydene.2015.01.132.

Moore, J. C. (1964) 'Gel permeation chromatography. I. A new method for molecular weight distribution of high polymers', *Journal of Polymer Science Part A: General Papers*, 2(2), pp. 835–843. doi: 10.1002/pol.1964.100020220.

Müller, K. and Arlt, W. (2013) 'Status and Development in Hydrogen Transport and Storage for Energy Applications', *Energy Technology*, 1(9), pp. 501–511. doi: 10.1002/ente.201300055.

Najjar, Y. S. H. (2013) 'Hydrogen safety: The road toward green technology', *International Journal of Hydrogen Energy*, 38(25), pp. 10716–10728. doi: 10.1016/j.ijhydene.2013.05.126.

Norris, I. D. *et al.* (2000) 'Electrostatic fabrication of ultrafine conducting fibers: Polyaniline/polyethylene oxide blends', *Synthetic Metals*, 114(2), pp. 109–114. doi: 10.1016/S0379-6779(00)00217-4.

Oka, K. *et al.* (2021) 'Synthesis of vinyl polymers substituted with 2-propanol and acetone and investigation of their reversible hydrogen storage capabilities', *Polymer Journal*, 53(7), pp. 799–804. doi: 10.1038/s41428-021-00475-1.

Orimo, S. I. *et al.* (2007) 'Complex hydrides for hydrogen storage', *Chemical Reviews*, 107(10), pp. 4111–4132. doi: 10.1021/cr0501846.

Panella, B., Hirscher, M. and Roth, S. (2005) 'Hydrogen adsorption in different carbon nanostructures', 43, pp. 2209–2214. doi: 10.1016/j.carbon.2005.03.037.

Ramachandran, R. and Menon, R. K. (1998) 'An overview of industrial uses of hydrogen', *International Journal of Hydrogen Energy*, 23(7), pp. 593–598. doi: 10.1016/s0360-3199(97)00112-2.

Reardon, H. *et al.* (2012) 'Emerging concepts in solid-state hydrogen storage: The role of

nanomaterials design', *Energy and Environmental Science*, 5(3), pp. 5951–5979. doi: 10.1039/c2ee03138h.

Ren, J. *et al.* (2016) 'ScienceDirect Current research trends and perspectives on materials-based hydrogen storage solutions : A critical review', *International Journal of Hydrogen Energy*, pp. 1–23. doi: 10.1016/j.ijhydene.2016.11.195.

Reneker, D. H. and Yarin, A. L. (2008) 'Electrospinning jets and polymer nanofibers', *Polymer*, 49(10), pp. 2387–2425. doi: 10.1016/j.polymer.2008.02.002.

Saeedmanesh, A., Mac Kinnon, M. A. and Brouwer, J. (2018) 'Hydrogen is essential for sustainability', *Current Opinion in Electrochemistry*, 12, pp. 166–181. doi: 10.1016/j.coelec.2018.11.009.

Sarfraz, A. *et al.* (2021) 'Electrode Materials for Fuel Cells', *Encyclopedia of Smart Materials*, 2, pp. 341–356. doi: 10.1016/B978-0-12-803581-8.11742-4.

Satyapal, S. *et al.* (2007) 'The U.S. Department of Energy's National Hydrogen Storage Project: Progress towards meeting hydrogen-powered vehicle requirements', *Catalysis Today*, 120(3-4 SPEC. ISS.), pp. 246–256. doi: 10.1016/j.cattod.2006.09.022.

Scanlon, L. G. *et al.* (2009) 'Hydrogen storage based on physisorption', *Journal of Physical Chemistry B*, 113(14), pp. 4708–4717. doi: 10.1021/jp809097v.

Sharma, S. and Ghoshal, S. K. (2015) 'Hydrogen the future transportation fuel: From production to applications', *Renewable and Sustainable Energy Reviews*, 43, pp. 1151–1158. doi: 10.1016/j.rser.2014.11.093.

Shiva Kumar, S. and Himabindu, V. (2019) 'Hydrogen production by PEM water electrolysis – A review', *Materials Science for Energy Technologies*, 2(3), pp. 442–454. doi: 10.1016/j.mset.2019.03.002.

Siegel, H. and Eggersdorfer, M. (2000) 'Ketones', in *Ullmann's Encyclopedia of Industrial Chemistry*. Weinheim, Germany: Wiley-VCH Verlag GmbH & Co. KGaA, pp. 560–579. doi: 10.1002/14356007.a15_077.

Simpson, A. J., Simpson, M. J. and Soong, R. (2018) 'Environmental Nuclear Magnetic Resonance Spectroscopy: An Overview and a Primer', *Analytical Chemistry*, 90(1), pp. 628–639. doi: 10.1021/acs.analchem.7b03241.

Singh, M. K. and Singh, A. (2022) 'Nuclear magnetic resonance spectroscopy', in *Characterization of Polymers and Fibres*. Elsevier, pp. 321–339. doi: 10.1016/B978-0-12-823986-5.00011-7.

Singla, M. K., Nijhawan, P. and Oberoi, A. S. (2021) 'Hydrogen fuel and fuel cell technology for cleaner future : a review', pp. 15607–15626.

Skoog, D. A., Holler, F. J. and Crouch, S. R. (2016) *Principles of Instrumental Analysis*. 7th edn, *Journal of the Spectroscopical Society of Japan*. 7th edn. Cengage Learning. doi: 10.5111/bunkou.9.181.

Spath, P. L. and Mann, M. K. (2003) *Life Cycle Assessment of Hydrogen production via Natural Gas Steam Reforming*.

Stankus, J. J. *et al.* (2006) 'Microintegrating smooth muscle cells into a biodegradable, elastomeric fiber matrix', *Biomaterials*, 27(5), pp. 735–744. doi: 10.1016/j.biomaterials.2005.06.020.

Tarasov, B. P. *et al.* (2021) 'Metal hydride hydrogen storage and compression systems for energy storage technologies', *International Journal of Hydrogen Energy*, 46(25), pp. 13647–13657. doi: 10.1016/j.ijhydene.2020.07.085.

Thompson, J. M. (2018) 'Some Fundamentals of Infrared Spectroscopy', in *Infrared Spectroscopy*. Jenny Stanford Publishing, pp. 1–33. doi: 10.1201/9781351206037-1.

Tomoda, B. T. *et al.* (2020) 'Characterization of biopolymer membranes and films: Physicochemical, mechanical, barrier, and biological properties', *Biopolymer Membranes and Films*, pp. 67–95. doi: 10.1016/b978-0-12-818134-8.00003-1.

Wang, Z. *et al.* (2016) 'Nitrogen-doped porous carbons with high performance for hydrogen storage', *International Journal of Hydrogen Energy*, 41(20), pp. 8489–8497. doi: 10.1016/j.ijhydene.2016.03.023.

Waters (2014) 'Styragel Column Care and Use Manual', *Waters Corporation*, pp. 1–11.

Williams, T. (1970) 'Gel permeation chromatography: A Review', *Journal of materials science*, 5(1), pp. 811–820. doi: 10.1016/0160-9327(84)90124-8.

Yadav, M. and Xu, Q. (2012) 'Liquid-phase chemical hydrogen storage materials', *Energy and Environmental Science*, 5(12), pp. 9698–9725. doi: 10.1039/c2ee22937d.

Yang, J. *et al.* (2010) 'High capacity hydrogen storage materials: Attributes for automotive applications and techniques for materials discovery', *Chemical Society Reviews*, 39(2), pp. 656–675. doi: 10.1039/b802882f.

Yasuda, I. *et al.* (2006) 'Development of membrane technology for highly-efficient hydrogen production', *16th World Hydrogen Energy Conference 2006, WHEC 2006*, 4(June), pp. 2754–2760.

Young, K. (2018) *Metal Hydrides, Chemistry, Molecular Sciences and Chemical Engineering*. Elsevier Inc. doi: 10.1016/B978-0-12-409547-2.05894-7.

Yu, H., Hebling, C. and Revathi, S. (2016) 'Fuel Cells: Microsystems', *Reference Module in*

Materials Science and Materials Engineering, (September 2015), pp. 1–15. doi: 10.1016/b978-0-12-803581-8.01727-6.

Zhao, H. *et al.* (2021) 'Raw biomass electroreforming coupled to green hydrogen generation', *Nature Communications*, 12(1), pp. 1–10. doi: 10.1038/s41467-021-22250-9.

Zhou, L. (2005) 'Progress and problems in hydrogen storage methods', *Renewable and Sustainable Energy Reviews*, 9(4), pp. 395–408. doi: 10.1016/j.rser.2004.05.005.

Zhu, Q. L. and Xu, Q. (2015) 'Liquid organic and inorganic chemical hydrides for high-capacity hydrogen storage', *Energy and Environmental Science*, 8(2), pp. 478–512. doi: 10.1039/c4ee03690e.

Zivar, D., Kumar, S. and Foroozesh, J. (2021) 'Underground hydrogen storage: A comprehensive review', *International Journal of Hydrogen Energy*, 46(45), pp. 23436–23462. doi: 10.1016/j.ijhydene.2020.08.138.

Züttel, A. (2004) 'Hydrogen storage methods', *Naturwissenschaften*, 91(4), pp. 157–172. doi: 10.1007/s00114-004-0516-x.

APPENDIX

APPENDIX

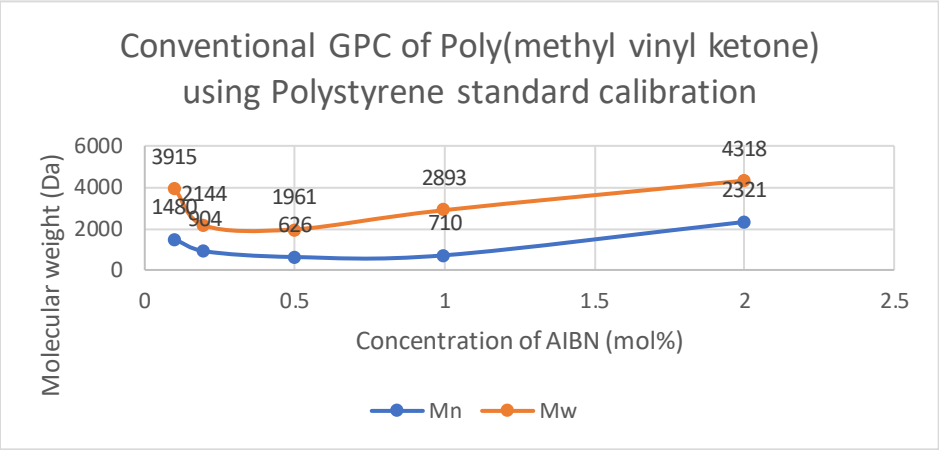

Figure A 1: GPC data of Poly(methyl vinyl ketone using polystyrene standard calibration

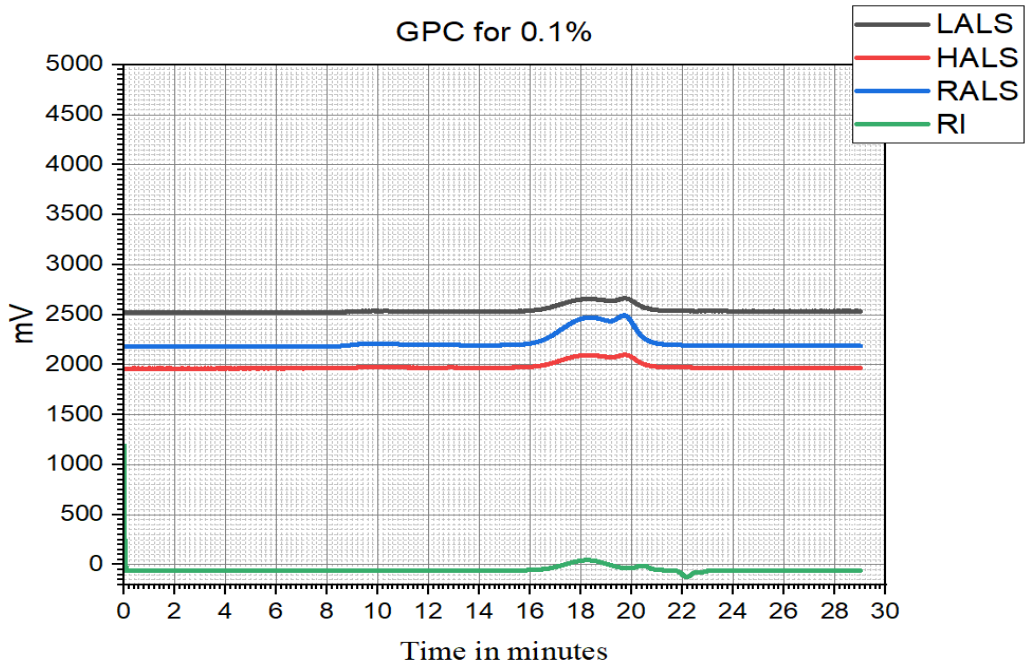

Figure A 2: Light scattering GPC data for PMVK synthesized with 0.1 mol% of AIBN

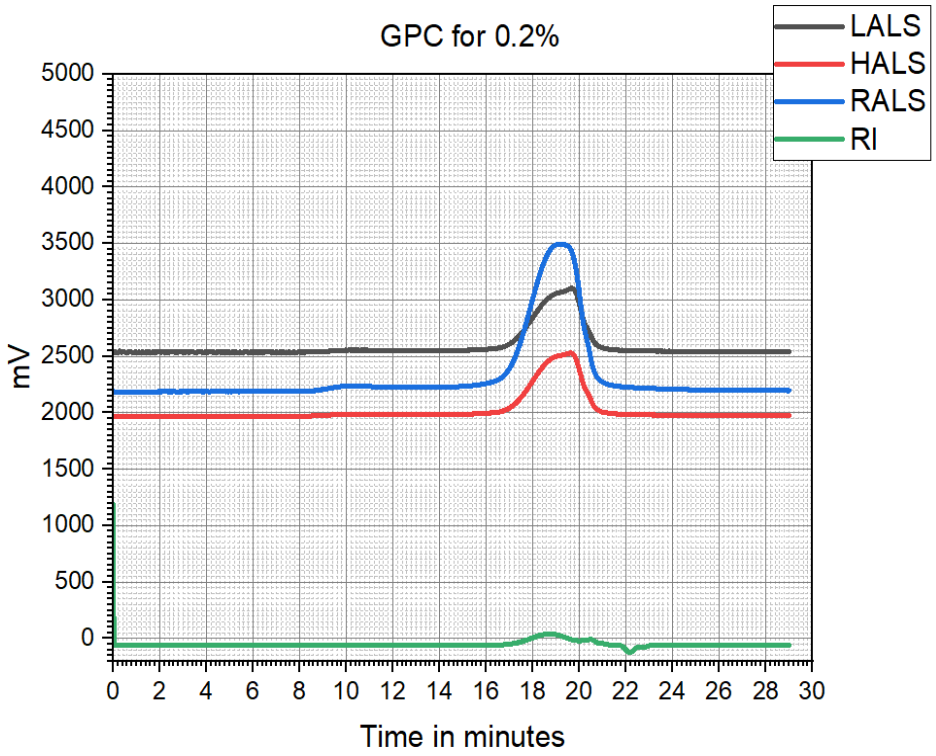

Figure A 3: Light scattering GPC data for PMVK synthesized with 0.2 mol% of AIBN

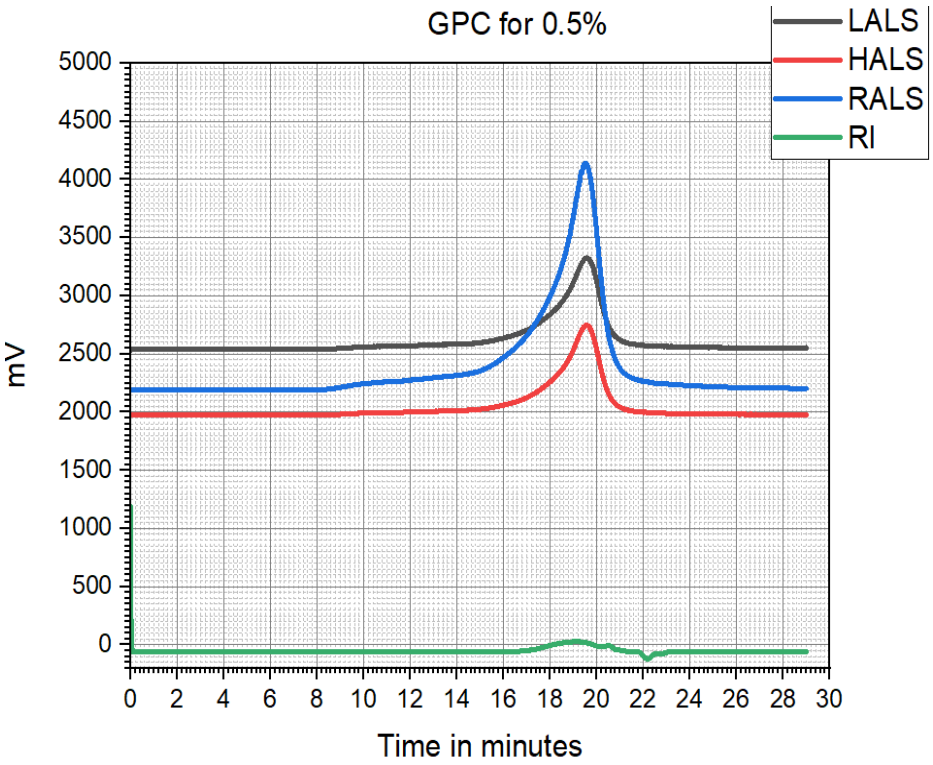

Figure A 4: Light scattering GPC data for PMVK synthesized with 0.5 mol% of AIBN

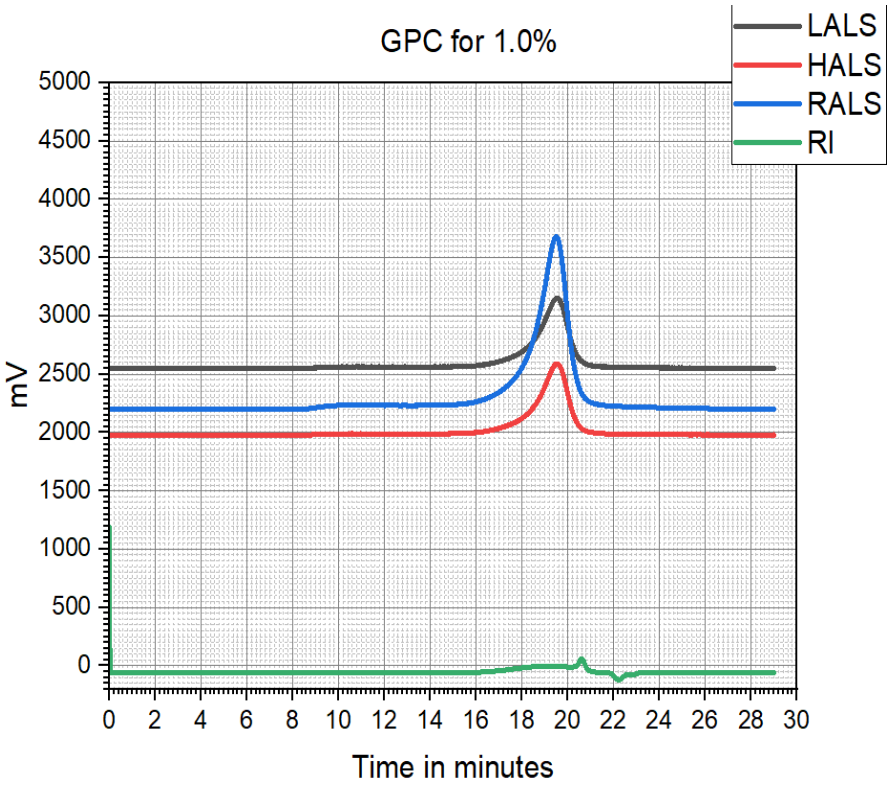

Figure A 5: Light scattering GPC data for PMVK synthesized with 1.0 mol% of AIBN

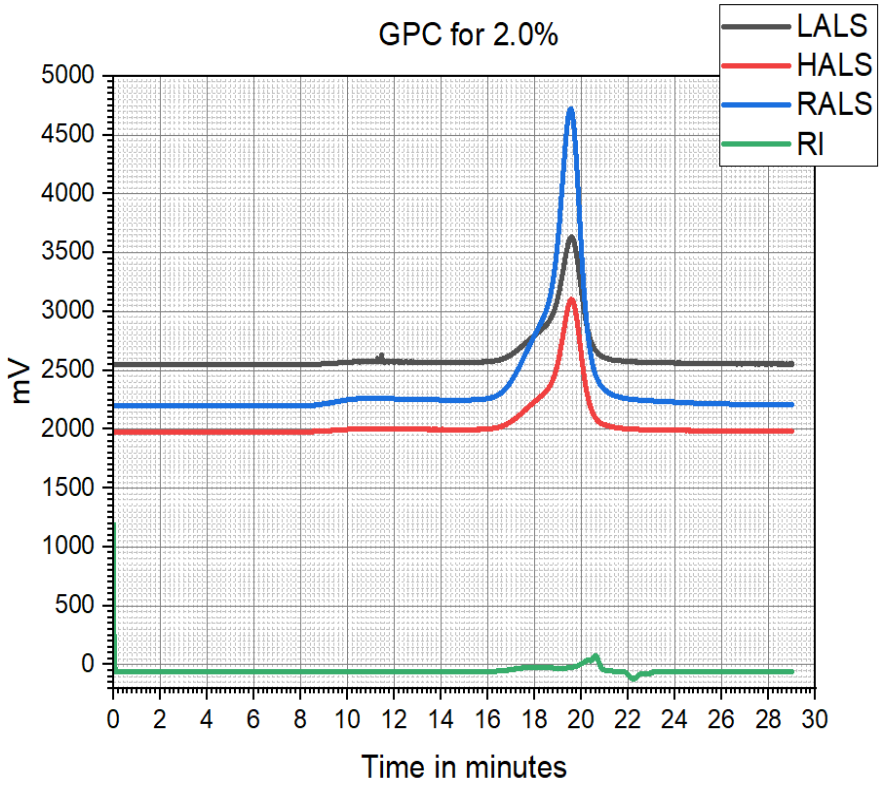

Figure A 6: Light scattering GPC data for PMVK synthesized with 2.0 mol% of AIBN

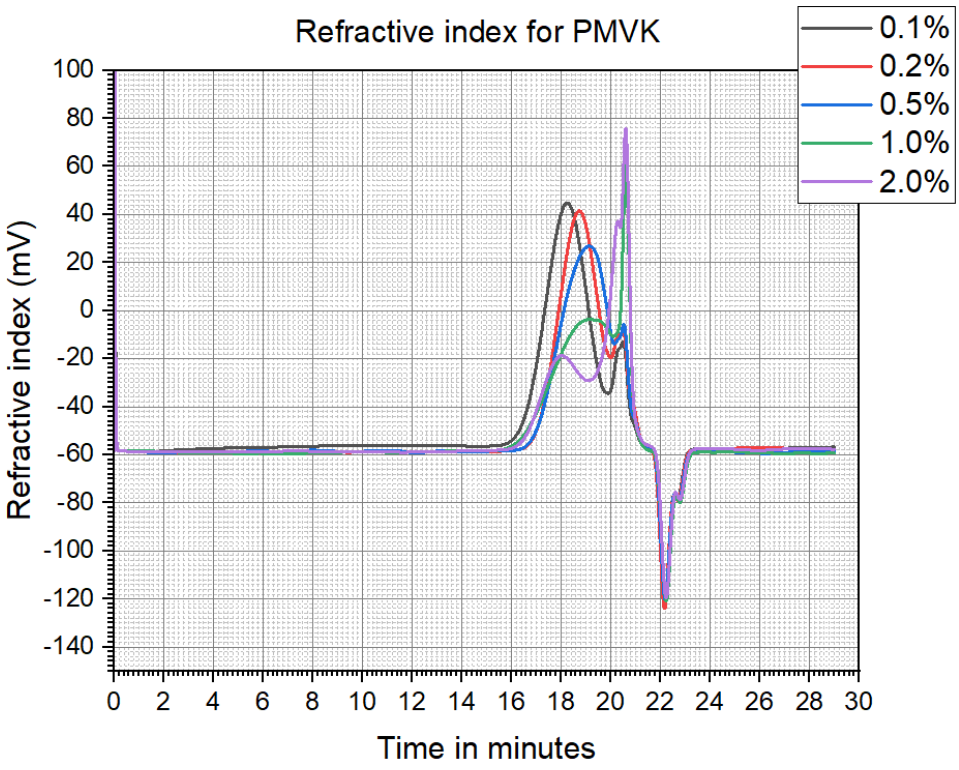

Figure A 7: Refractive index vs elusion time for PMVK

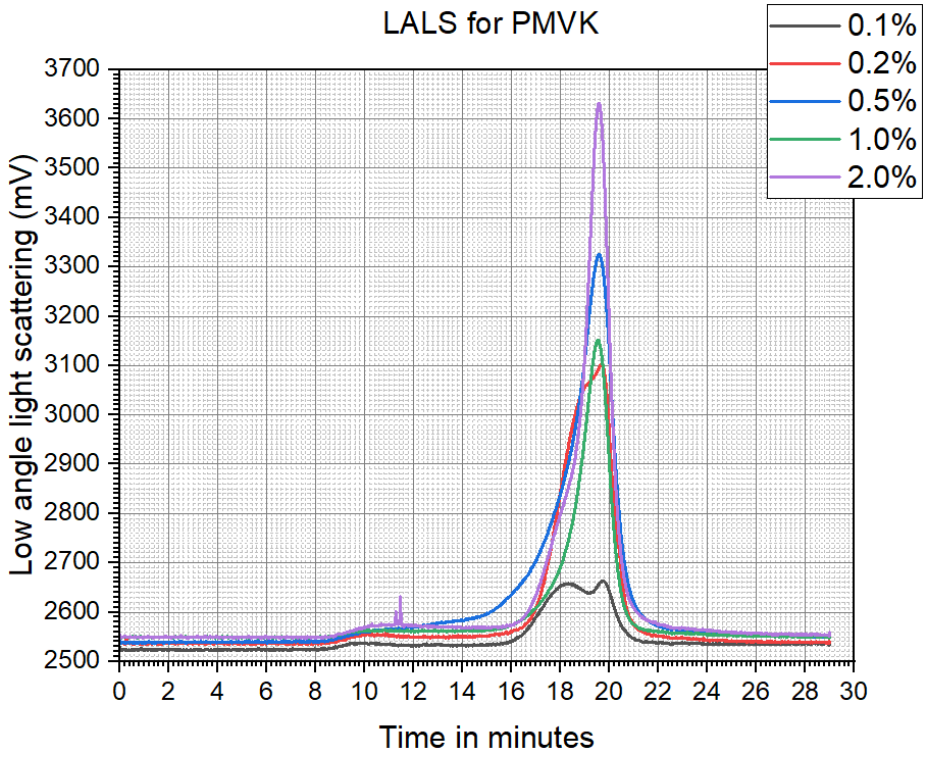

Figure A 8: LALS vs elusion time for PMVK

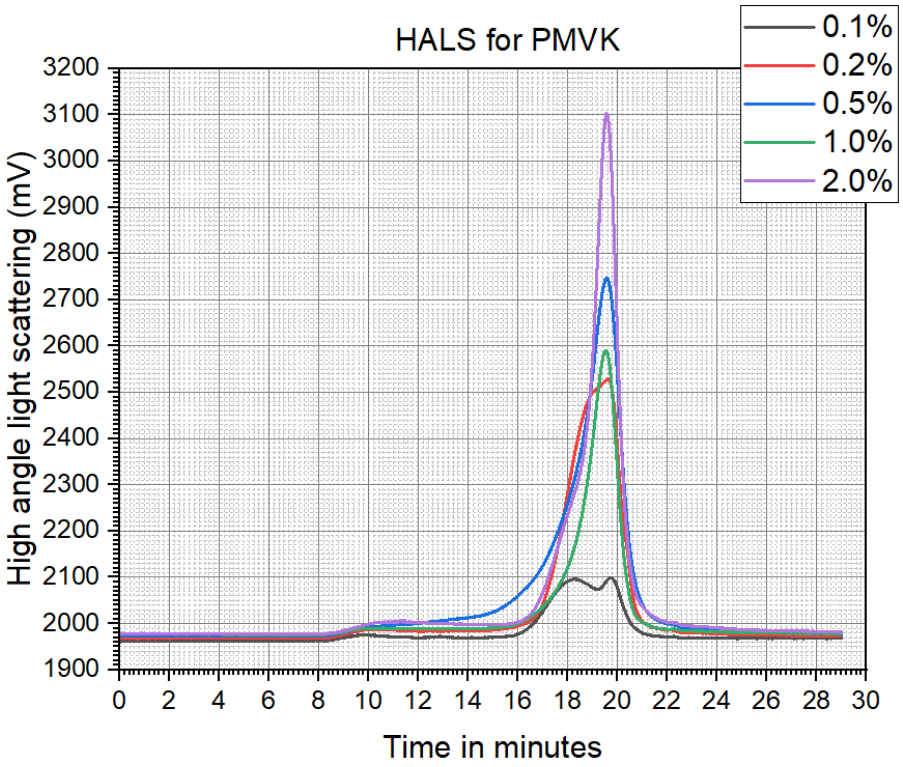

Figure A 9: HALS vs elusion time for PMVK

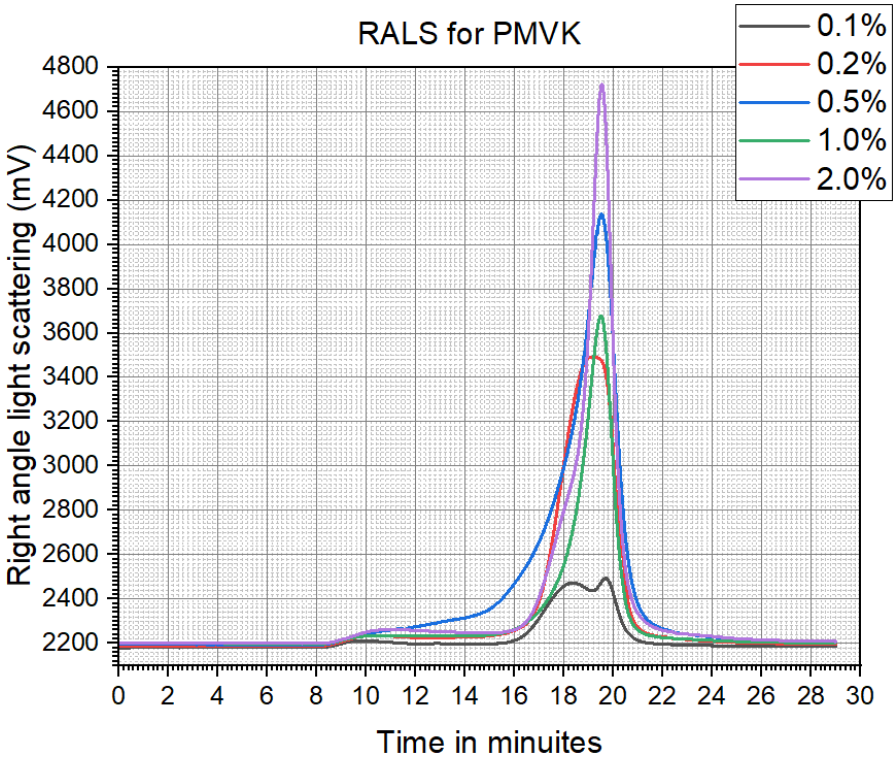

Figure A 10: RALS vs elusion time for PMVK

BIOGRAPHICAL SKETCH

Dominic Adrewie was born in Accra, Ghana on the 2nd of May 1995. In 2008, he earned a Bachelor of Science in Chemistry from the Kwame Nkrumah University of Science and Technology in Ghana. He began his Master of Science degree in Chemistry at the University of Texas Rio Grande Valley (UTRGV) in Edinburg, Texas, in Spring 2021 and was awarded the Presidential Graduate Research Assistantship (PGRA) by UTRGV for the duration of his studies. His research concentrated on the synthesis and processing of polymers for use in hydrogen storage. He worked under the guidance of Dr. Javier Macossay-Torres and in August of 2022, he received his Master of Science degree in Chemistry after fulfilling all requirements.

Author can be reached via email at:

dominic.adrewie01@utrgv.edu or dominicsaved@gmail.com